

# Fate modeling of nonylphenol ethoxylates and their metabolites in the Dutch Scheldt and Rhine estuaries: validation with new field data

Niels Jonkers<sup>a</sup>, Remi W.P.M. Laane<sup>b</sup>, Chris de Graaf<sup>a</sup>, Pim de Voogt<sup>a,\*</sup>

<sup>a</sup>*Department of Environmental and Toxicological Chemistry, Institute for Biodiversity and Ecosystem Dynamics, University of Amsterdam, Nieuwe Achtergracht 166, 1018 WV Amsterdam, The Netherlands*

<sup>b</sup>*National Institute for Coastal and Marine Management/RIKZ, Kortenaerkade 1, 2518 AX The Hague, The Netherlands*

Received 21 January 2004; accepted 24 August 2004

## Abstract

The environmental behavior of nonylphenol ethoxylates (A<sub>9</sub>PEO) in the Rhine and Scheldt estuaries (The Netherlands) was investigated using a hydrodynamic advection-dispersion fate model (ECoS 3). The model was validated with the results of field studies, in which A<sub>9</sub>PEO as well as the metabolites nonylphenoxy ethoxy acetic acids (A<sub>9</sub>PEC) and nonylphenol (NP) were analyzed in sediment, water and suspended particulate material (SPM) samples using LC-MS methods. Maximum actual concentrations observed in surface sediments were 620, 560 and 1100 ng g<sup>-1</sup> d.w. for A<sub>9</sub>PEO, A<sub>9</sub>PEC and NP, respectively. In the dissolved phase, maximum observed concentrations amounted to 1100 ng L<sup>-1</sup> (A<sub>9</sub>PEO), 6500 ng L<sup>-1</sup> (A<sub>9</sub>PEC) and 960 ng L<sup>-1</sup> (NP). Clear spatial trends were observed for dissolved A<sub>9</sub>PEO and metabolites in the Scheldt estuary, with decreasing concentrations going downstream. This concentration decrease was steeper than for conservatively behaving compounds. This trend was not visible in the Rhine estuary. The fate model was applied to A<sub>9</sub>PEO and metabolites in both estuaries. Transport of chemicals in the water column was considered as a longitudinal one-dimensional process through a number of estuary segments. For the Rhine estuary, to cope with the stratification observed, a model structure was chosen consisting of two water layers above each other, between which exchange was possible. Sedimentation/erosion processes were included in the model. A biodegradation scheme was incorporated, and rates were adjusted to fit the calculated concentration profiles with the actual profiles of both A<sub>9</sub>PEO and its metabolites. In this way, field biodegradation rates for A<sub>9</sub>PEO, A<sub>9</sub>PEC and NP could be derived, which were in agreement with values from literature. The measured dissolved concentration profiles as well as salinity and concentrations of SPM could be described successfully by the model. The concentrations calculated in SPM and sediment were of the same order of magnitude as the actual concentrations. In the Rhine estuary, additional sources of A<sub>9</sub>PEO had to be included to account for the relatively high concentrations in the middle of the estuary. The fate model for the Scheldt estuary could be slightly improved by using salinity-dependent biodegradation rates. A sensitivity analysis of the model showed that in the Scheldt estuary, the environmental process with the strongest influence on the dissolved concentration profiles of A<sub>9</sub>PEO and metabolites is biodegradation. In the Rhine estuary, the water residence time is too short for significant biodegradation to occur, and in this estuary the dissolved concentration profiles were mainly influenced by the additional A<sub>9</sub>PEO sources.

© 2004 Elsevier Ltd. All rights reserved.

**Keywords:** surfactant; nonylphenol ethoxylate; nonylphenoxy ethoxy acetic acid; estuaries; fate model

\* Corresponding author.

E-mail address: [pdevoogt@science.uva.nl](mailto:pdevoogt@science.uva.nl) (P. de Voogt).

## 1. Introduction

The nonionic surfactants nonylphenol ethoxylates ( $A_9PEO$ ) receive a lot of scientific attention, because of their excellent surface active properties as well as their potential environmental risk.  $A_9PEO$  have a worldwide production of around 700,000 tons annually and are used in a wide range of applications. Their main application is as industrial and institutional (30%) or household (15%) cleaning agent (Ying et al., 2002; Knepper and Berna, 2003). The remaining  $A_9PEO$  is used in many industrial applications, e.g. as wetting agents, dispersants, emulsifiers, solubilizers, foaming agents and polymer stabilizers (Ying et al., 2002).  $A_9PEO$  reach the environment mainly via wastewater treatment plants.

Although the environmental behavior of  $A_9PEO$  has been extensively studied in recent years, the environmental risk of these compounds is still a subject of debate. The environmental concern for these compounds is mainly because of the endocrine disrupting effects of two short-chain  $A_9PEO$  oligomers ( $A_9PEO_1$  and  $A_9PEO_2$ ) and the metabolite nonylphenol (NP) (Jobling and Sumpter, 1993; Legler et al., 1999). In the European Union, these concerns have led to a EU Directive on the restriction of the use of NP and APEO in applications in which these compounds may end up in wastewater (Cox and Drys, 2003). No regulatory action has been taken in the USA yet.

The environmental presence of  $A_9PEO$  and NP has been established in both sediment, water and suspended particulate material in freshwater (Bennie, 1999), marine (Petrovic et al., 2002; Heemken et al., 2001) and estuarine environments (Kveřtak et al., 1994; Ferguson et al., 2001; Marcomini et al., 2000; Jonkers et al., 2003). Field sorption coefficients show  $\log K_{oc}$  ranges of 5.4–6.0 (NP)

and 4.9–6.4 ( $A_9PEO$ ) (Ferguson et al., 2001; Heemken et al., 2001; Jonkers et al., 2003).

One of the uncertainties in the environmental fate of  $A_9PEO$  is their biodegradation behavior. Two biodegradation routes are known for these compounds, as shown in Fig. 1. In the oxidative-hydrolytic pathway, the main metabolites are the alkylphenoxy ethoxy acetic acids ( $A_9PEC$ ), followed by the doubly oxidized CAPEC metabolites (DiCorcia et al., 1998; Jonkers et al., 2001). This degradation route is mainly observed in freshwaters (Jonkers et al., 2001). The nonoxidative hydrolytic pathway results in short-chain  $A_9PEO$  and NP. This route is mainly followed in marine waters and sediments. Shang et al. (1999) reported that biodegradation rates in marine sediments are extremely slow. In another study, both short and long chain  $A_9PEO$  were reported in marine sediments, indicating that biodegradation does occur to some extent in this compartment (Jonkers et al., submitted for publication). In estuarine environments, biodegradation by both the oxidative and the nonoxidative route have been reported (Marcomini et al., 2000; Jonkers et al., 2003).

The relevance of the metabolites of  $A_9PEO$  was recently demonstrated by Fenner et al. (2002), who showed in an environmental risk assessment of the mixture of  $A_9PEO$ ,  $A_9PEC$  and NP that the metabolites accounted for 89% of the overall risk.

In a field study in the Scheldt estuary (The Netherlands),  $A_9PEO$  concentration profiles showed a faster than conservative concentration decrease during transport through the estuary (Jonkers et al., 2003). In addition, the ratios of metabolites over surfactant gradually increased when going downstream, indicating that biodegradation is proceeding in the estuary. However, from those results it is not possible to directly derive

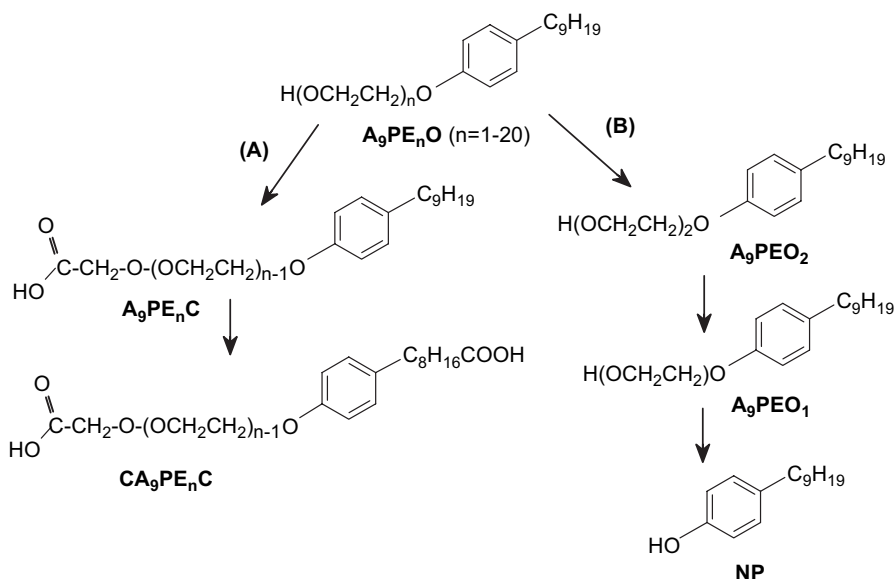


Fig. 1. Biodegradation routes of  $A_9PEO$ : the oxidative hydrolytic pathway (A) and the non-oxidative hydrolytic pathway (B).

field biodegradation rate constants for A<sub>9</sub>PEO, as it is difficult to quantitatively determine the contribution of dilution, biodegradation and sorption processes.

Application of an environmental fate model can provide a more quantitative insight into the importance of the different environmental processes which influence the fate of A<sub>9</sub>PEO in estuaries. To the best of our knowledge, the few fate modeling studies on surfactants in the literature are limited to the anionic linear alkylbenzene sulfonates (LAS) (Amano et al., 1991; Morioka and Chikami, 1986). A generic mathematical fate model applied to LAS in a Japanese estuary showed that biodegradation is by far the most important removal process in summer, while in winter, biodegradation and sedimentation processes had an equal contribution to the disappearance of LAS from the water column (Amano et al., 1991). For Tokyo Bay and Osaka Bay (Japan), two hydraulic mass balance models were constructed for LAS, showing that the dominating removal processes were biodegradation and tidal transport out of the area (Morioka and Chikami, 1986).

No previous studies exist in which environmental fate models are applied to nonionic surfactants. Only for the metabolite nonylphenol, a box model using a mass balance approach was constructed for its fate in the Hudson estuary (USA) (Van Ry et al., 2000).

In the present study, a fate model is constructed for A<sub>9</sub>PEO in the Scheldt and Rhine estuaries, two heavily industrialized areas in the Netherlands (see Fig. 2). This study makes use of the ECoS modeling software (version 3.0, Plymouth Marine Laboratory, UK), which has been applied to several other estuarine systems. In the Tamar estuary (UK), the distribution of Zn and Ni in the dissolved and suspended particulate phase was described (Liu et al., 1998), while in the Gironde estuary (France) the distribution of dissolved Cd was modeled (Pham et al., 1997).

Fate models for the Scheldt and Rhine estuaries have been used in the past for other compounds. A one-dimensional hydrological model using ECoS3 software was able to describe the general movement of water masses in the Scheldt estuary, as well as the dissolved

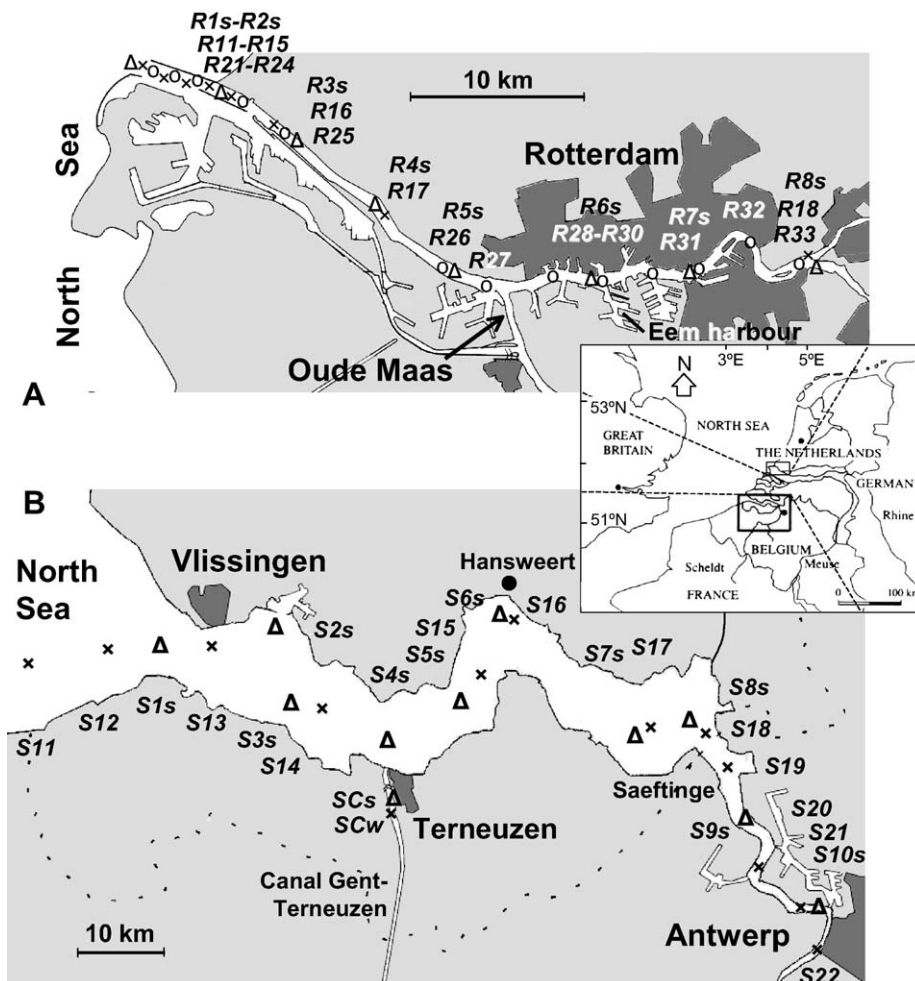


Fig. 2. Map of the study areas Rhine (A) and Scheldt (B) estuary, with sampling locations. x = water 2000; Δ = sediment 2000; ○ = water 2002.

concentration profiles of a number of pesticides (Steen et al., 2002). The model was based on the earlier SAWES model (Systems Analysis WEstern Scheldt), which was developed by Van Gils et al. (1993). The SAWES model was used by Zwolsman to describe the concentration profiles and speciation of some trace metals in the Scheldt estuary (Zwolsman, 1999). For the fate modeling of PCB in the Scheldt estuary, a general water quality model named WASP has been used (Vuksanovic et al., 1996). According to that model, the distribution of PCB was mainly regulated by hydrophobic sorption and suspended sediment transport.

In the Rhine estuary, hydrological fate models have been used for the study of trace metals, benzo[*a*]pyrene and oil in harbor sediments (Boderie and Sonneveldt, 1996). In that study, important contaminant sources besides the Rhine river itself were industrial discharges for the metals and oil, and shipping activity for benzo[*a*]pyrene and oil.

### 1.1. Objective

This research aims to describe the sources, fate and distribution of A<sub>9</sub>PEO surfactants and their metabolites in the two Dutch estuaries Rhine and Scheldt by using a hydrological fate model. New field data are presented which, combined with already published results, were used for validation of the model.

A main objective in this model study was to obtain a quantitative estimate of A<sub>9</sub>PEO biodegradation rates, as it is difficult to estimate this environmental process directly from field data or laboratory experiments. By fitting the biodegradation rate constants to the concentration profiles observed for both A<sub>9</sub>PEO and its metabolites, a quantitative estimation could be made of the biodegradability of these compounds in the field.

## 2. Methods

### 2.1. Study areas

The two investigated areas are both situated in the south of The Netherlands, as shown in Fig. 2.

The first study area is the Western Scheldt estuary, which is 100 km long with a strong curvature, and has a width of 500 m at Antwerp and 6500 m at Vlissingen. The mesotidal estuary has a freshwater input from the Scheldt river of on average  $104 \text{ m}^3 \text{ s}^{-1}$ . The water in the estuary has a residence time of two to three months and is vertically well-mixed. An additional source of freshwater to the estuary is the canal Gent–Terneuzen (on average  $15 \text{ m}^3 \text{ s}^{-1}$ ). The main industrial areas are the harbors of Antwerp and Vlissingen (Baeyens et al., 1998).

A strong exchange of material between sediment and suspended particulate material (SPM) occurs in the

Scheldt estuary. It is estimated that a sediment surface layer of 0.5 m in the entire estuary is mixed into the water column every 0.5 year (Van Maldegem et al., 1993). About 90% of the terrestrial SPM which enters the Scheldt estuary is retained there (Baeyens et al., 1998). The most important sedimentation area is the tidal marshland Saeflinge. The shipping channel of the Scheldt estuary is heavily dredged, and the dredged material is dumped elsewhere in the estuary.

The other investigated area is the Rhine estuary, which passes the harbors of Rotterdam. The length of the estuary is 40 km, with an average width of around 500 m. The freshwater input is around  $800 \text{ m}^3 \text{ s}^{-1}$  at the head of the estuary, while halfway the estuary the river Oude Maas provides another large freshwater input of  $700 \text{ m}^3 \text{ s}^{-1}$ . The residence time of the water in the estuary is between one and three days, and the water column is vertically stratified. It is estimated that the retention of riverine SPM in the Rhine estuary is about 50% (Laane, unpublished results). The whole estuary is heavily industrialized, and has intensive shipping traffic. Due to heavy dredging activities and strong tidal currents in the estuary, the surface sediment layer is well-mixed (Eisma et al., 1982).

### 2.2. Sampling strategy

Two sampling campaigns were performed in the Scheldt estuary, in November 1999 and June 2000. In the Rhine estuary, three sampling campaigns were conducted, in December 1999, September 2000, and October 2002. Results of both campaigns of 1999 were previously reported (Jonkers et al., 2003).

Sampling locations for surface sediments were evenly distributed over the entire estuary (see Fig. 2). Three box cores (average core depth 30 cm) were collected at each location and the complete cores were mixed, in order to obtain a sample representative of the location. Water samples were taken along the salinity gradient, at 2‰ salinity intervals (monitored on-line during the sampling campaigns). As a consequence, water sampling locations are different from those of the sediments. In the Scheldt estuary, additional water, SPM and sediment samples were collected just inside the canal Gent–Terneuzen.

Water sampling techniques were different for the different sampling campaigns. In both campaigns of 1999, samples were taken from the water surface (at a depth of approximately 0.5 m) using a stainless steel bucket. In the campaigns of 2000, a water sampling torpedo was used, which obtained water at 1.5 m depth.

For the 2002 campaign in the Rhine estuary, both sampling techniques were used at each sampling location, with one water sample taken with a bucket from the water surface, a second sample taken at 1.5 m depth using the sampling torpedo, and a third sample taken at the maximum depth the sampling torpedo could reach

(between 2.7 and 6.7 m). The goal of this extensive sampling was to obtain insight into the vertical distribution of A<sub>9</sub>PEO in the salinity stratified water column of this estuary. In addition to the samples taken along the salinity gradient, in the 2002 campaign samples were also collected in (locations R27, R29 and R30) and between (R26, R28 and R31) the exits of the main harbors of the Rhine estuary, to investigate the contribution of the harbors to the concentration profiles observed in the estuary. No sediments or SPM samples were collected during that campaign.

### 2.3. Analysis

The extraction procedures and LC–MS analysis of the water, SPM and sediment samples have been described in detail elsewhere (Jonkers et al., 2003).

Briefly, water samples were filtered and the glass-fiber filters (GF/C, pore size 1.2 μm) were extracted separately. Filtered water was acidified and extracted using Solid-Phase Extraction (SPE) with a C<sub>18</sub>-SPE cartridge. Cartridges were eluted with methanol. Water samples were extracted immediately on board the sampling ship to avoid any possible conservation problems. Sediment samples were frozen until further treatment in the laboratory.

Wet sediment samples and filters (SPM samples) were Soxhlet extracted overnight with basic methanol. The extract was concentrated, nanopure water was added and this mixture was acidified and cleaned up using SPE as described above.

A<sub>9</sub>PEO<sub>2</sub> and NP labeled with <sup>13</sup>C-labeled aromatic rings were added as internal standards. Analysis was performed using reversed phase liquid chromatography coupled to electrospray mass spectrometry detection, as described previously (Jonkers et al., 2003). Analyses were done in SIM mode, using positive ionization for A<sub>9</sub>PEO, and negative ionization for A<sub>9</sub>PEC and NP. The oligomers A<sub>9</sub>PEO<sub>1</sub> and A<sub>9</sub>PEO<sub>2</sub> were quantified separately with pure standards, while the longer oligomers were quantified together using a commercial standard mixture of on average 10 ethoxylate units. For NP, A<sub>9</sub>PE<sub>1</sub>C and A<sub>9</sub>PE<sub>2</sub>C pure standards were available (see structures in Fig. 1), and for longer A<sub>9</sub>PE<sub>>2</sub>C oligomers, the calibration of A<sub>9</sub>PE<sub>2</sub>C was used (Jonkers et al., 2003).

### 2.4. Fate model structure

The field data showed the analytes to be present in relevant concentrations in both the water, suspended particulate material and sediment compartments. Therefore, all three compartments are incorporated into the fate model. It is assumed that no atmospheric exchange takes place in the estuaries. For A<sub>9</sub>PEO (Henry coefficient of 0.0003 Pa m<sup>3</sup> mole<sup>-1</sup> for A<sub>9</sub>PEO<sub>2</sub>) and A<sub>9</sub>PEC, this seems reasonable. NP (Henry coefficient 0.6 Pa m<sup>3</sup>

mole<sup>-1</sup>) is more volatile, and therefore it cannot be completely ruled out that some atmospheric exchange occurs for this compound (Van Vlaardingen et al., 2003). A study of the estuarine fate of alkylphenols in the Hudson Bay by Van Ry et al. (2000) did suggest that atmospheric exchange is a relevant process for NP. However, due to a complete lack of data on the atmospheric presence of NP in the investigated estuaries, this process was not yet incorporated into the model.

The description of the water movement was based on the actual geographies of the estuaries and on actual hydrological data. Exchange processes of analytes between water and SPM (sorption) and of SPM with sediment (sedimentation/erosion) were incorporated. For the stratified Rhine estuary, exchange of dissolved analytes and SPM between the upper and lower water layer was included as well. In addition, biodegradation was incorporated into the model.

For modeling purposes, A<sub>9</sub>PEO and their metabolites were divided into the following groups: A<sub>9</sub>PEO<sub>>2</sub>, A<sub>9</sub>PEO<sub>1,2</sub>, A<sub>9</sub>PE<sub>>2</sub>C, A<sub>9</sub>PE<sub>1,2</sub>C and NP. One reason for this division was the fact that the short-chain A<sub>9</sub>PEO<sub>1,2</sub> are considered as metabolites of the long chain A<sub>9</sub>PEO<sub>>2</sub> in the non-oxidative hydrolytic pathway. In addition, it is interesting to consider the fate and behavior of these two oligomers separately from a toxicological point of view, as these short-chain A<sub>9</sub>PEO<sub>1,2</sub> are the only endocrine disrupting oligomers.

The software used in this study is the ECoS 3.0 modeling framework. This software is specifically designed to model physical, chemical and biological processes in estuaries. The scheme in Fig. 3 shows the structure and input parameters of the model.

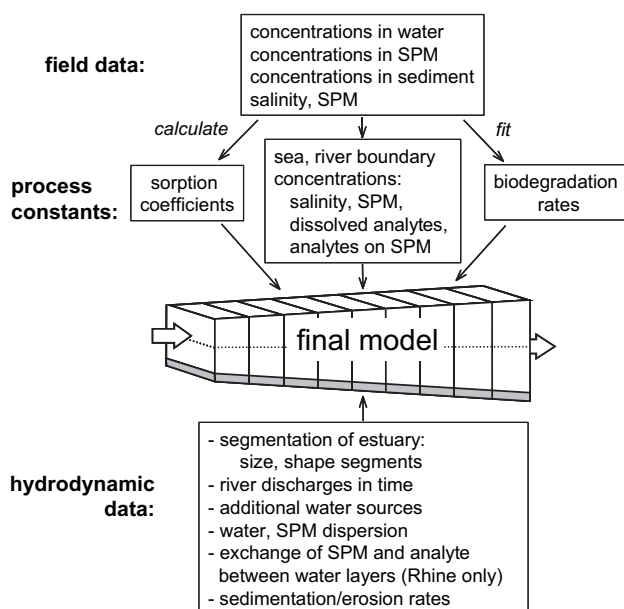


Fig. 3. Scheme of the ECoS model, showing the required input data.

Optimization of the model was first done using the data of the sampling campaign in the Scheldt estuary of 1999, as those results showed the smoothest dissolved concentration profiles and were therefore easiest to work with. Then, the model was adjusted to optimize it for the data sets of the other campaigns.

In the ECoS modeling framework, it is necessary to define boundary conditions of the model space (analyte concentrations, salinity and SPM at the river and open sea end of the estuary). These boundaries were fixed at the actual concentrations measured in the field samples. In order to fit the data of the different sampling campaigns, the model scenarios were run separately, using boundary concentrations corresponding to the actual concentrations at the time of sampling. It was assumed that the fluctuation of the analyte concentrations at the boundaries is relatively small.

### 3. Results and discussion

#### 3.1. Model optimization

##### 3.1.1. Hydrology

For both the Scheldt and Rhine estuary, data on actual freshwater input at the head of the estuaries were provided by the Dutch Ministry of Transport, Public Works and Water Management. Ten-day average values were used in the Scheldt model, while in the Rhine estuary 5-day averaged input values were used. For the Rhine estuary, actual data on the input of the additional freshwater source the river Oude Maas were also incorporated into the model using 5-day average values. In the Scheldt estuary, the additional freshwater input of the canal Gent–Terneuzen was fixed at the average value of  $10 \text{ m}^3 \text{ s}^{-1}$ .

To describe the actual shape of the estuaries, they were divided into a number of segments, each with their known depth, width and cross-sectional area. Transport of chemicals in the water column is considered as a longitudinal one-dimensional process described by the advection-dispersion equation proposed by Pritchard (1958). For the derivation of the dispersion coefficients ( $K_x$ ) between the water segments, the dilution profile of the conservatively behaving salinity was used. The assumption is made that the salinity gradient is in steady state, that is the advection and dispersion balance each other. With an integrated version of the advection-dispersion equation,  $K_x$  values can be determined for any position in the estuary from the slope of the plot of salinity against distance (Steen et al., 2002).

The Scheldt estuary was divided into 19 segments of around 5 km and treated as vertically well-mixed (Van Gils et al., 1993; Baeyens et al., 1998). These data were taken from the study by Steen et al. (2002), and were originally derived from the SAWES model (Van Eck and De Rooij, 1990).

The optimized dispersion coefficients for the segments of the Scheldt estuary ranged from  $86$  to  $335 \text{ m}^2 \text{ s}^{-1}$ , and are in the same range as values reported in literature for this estuary (Soetaert and Herman, 1995; Vuksanovic et al., 1996; Steen et al., 2002). Fig. 4a shows the calculated salinity curve obtained with this method. When the  $K_x$  values optimized for the 1999 sampling campaign were used to describe the salinity curve of the 2000 sampling campaign, an acceptable fit was obtained as well. The description of salinity in time was also modeled correctly, as can be seen in Fig. 4b, which shows the calculated and actual salinities at three locations in the Scheldt estuary over a period of 700 days.

The segmentation and segment geometries of the Rhine estuary were based on the DELWAQ model

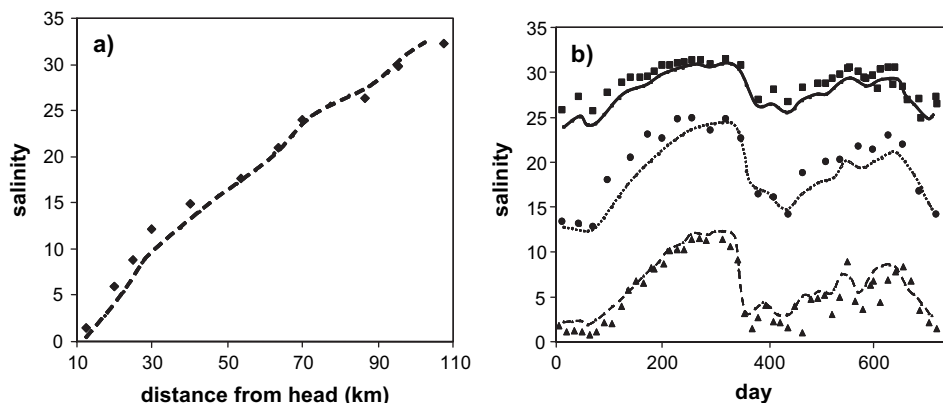


Fig. 4. (a) Calculated and actual salinity profiles for the Scheldt estuary data of 1999. ◆, actual salinities; striped line, calculated salinity profile. (b) Calculated and actual salinities at three locations in the Scheldt estuary during 700 days (day 1 is January 1, 1999). ■, actual salinity at  $x = 95$  km; full line, calculated salinity at  $x = 95$  km; ●, actual salinity at  $x = 70$  km; dotted line, calculated salinity at  $x = 70$  km; ▲, actual salinity at  $x = 37$  km; striped line, calculated salinity at  $x = 37$  km.

(Boderie and Sonneveldt, 1996). This estuary was divided into 42 segments of approximately 1 km length each. The vertical stratification of the water column was incorporated into the model by horizontally dividing all segments of the Rhine estuary into equal surface and bottom layers, between which exchange of matter was possible.

As the field data (see Section 3.2.3) showed that the concentrations in the surface layer were on average higher by a factor of 2.5 than in the bottom layer, the exchange between the two layers was programmed to be at equilibrium when this ratio was reached. In addition, as the field data showed a stronger stratification of analyte concentrations in the saline region, the equilibrium ratio was made salinity dependent. Stratification of A<sub>9</sub>PEO and NP in an estuarine water column was previously reported for the Krka estuary (Croatia) by Kveštak et al. (1994).

Water dispersion coefficients for the Rhine estuary were again determined from the salinity profiles in the estuary. Two separate series of  $K_x$  values were optimized, because the salinity profiles of the surface and bottom water layers were different. As the salinities in the upstream part of the estuary were close to 0, in that region moderate  $K_x$  values of  $250 \text{ m}^2 \text{ s}^{-1}$  were chosen. At the saline end of the estuary, for some segments relatively high  $K_x$  values (up to  $800 \text{ m}^2 \text{ s}^{-1}$ ) were necessary to describe the salinity profiles. With moderate  $K_x$  values, the modeled salt intrusion would be significantly smaller than observed in the field. A comparison of the calculated and actual salinities during the 2002 sampling campaign in the Rhine estuary (surface and maximum depth samples only) is shown in Fig. 5.

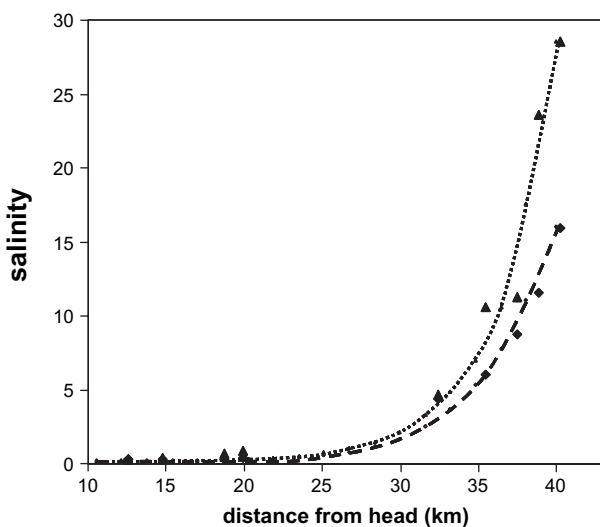


Fig. 5. Calculated and actual salinity profiles for the Rhine data of 2002. ◆, actual salinities in surface water layer; striped line, calculated salinity profile surface layer; ▲, actual salinities in bottom water layer; dotted line, calculated salinity profile bottom layer.

### 3.1.2. Suspended particulate material

The movement of SPM in the horizontal direction was described by advection and dispersion, while for movement in the vertical direction, sedimentation and erosion were incorporated into the model.

Downstream movement of SPM is the result of advective movement with the water, and therefore increases with water velocity ( $U_w$ ). A contrary process occurs due to the asymmetry between the rise and fall of the tide caused by frictional dissipation of tidal energy, causing a more rapid flood and a slower ebb in the estuary, which results in an upstream transport of SPM. Therefore, the velocity of SPM ( $U_{x,\text{spm}}$ ) was simulated to increase with water velocity, and decrease with tidal range ( $R$ ) and salinity ( $S$ ), according to the equation  $U_{x,\text{spm}} = a_1 * U_w - b_1 * R * S$  (Harris and Gorley, 1998).

Dispersion of the SPM ( $K_{x,\text{spm}}$ ) increased with both water velocity, the tidal range and salinity, via the equation  $K_{x,\text{spm}} = a_2 * U_w - b_2 * R * S$ .

With these equations, a turbidity cloud is present when  $U_{x,\text{spm}} = 0$ , or when  $a_1 * U_w = b_1 * R * S$ . The location of this maximum can be shifted by changing coefficients  $a_1$  and  $b_1$ . In the Scheldt estuary model,  $a_1$  and  $b_1$  are adjusted so that  $U_{x,\text{spm}} = 0$  at  $x = 20 \text{ km}$ , as it is known from literature the turbidity cloud in the Scheldt estuary occurs in that region at average river discharge (Vuksanovic et al., 1996).

For the Scheldt estuary, the sedimentation and erosion rates of SPM were fitted to both the observed SPM concentration profile in the estuary and the average analyte concentrations in both compartments. Exchange of SPM with the surface sediment was estimated by Van Maldegem et al. (1993) to be between  $0.1$  and  $1 \text{ kg m}^{-2} \text{ day}^{-1}$  for the whole Scheldt estuary. In this study, a default value of  $0.17 \text{ kg m}^{-2} \text{ day}^{-1}$  ( $0.002 \text{ g m}^{-2} \text{ s}^{-1}$ ) was chosen for both sedimentation and erosion. To optimize the fit of the SPM concentration profile, sedimentation or erosion fluxes were adjusted in certain areas of the estuary (Van Maldegem et al., 1993). According to Van Maldegem et al. (1993), the net sedimentation is highest at Saeftinge ( $x = 35\text{--}45 \text{ km}$ ), and close to zero around Antwerp. In the downstream section of the estuary, an area with net resuspension is present. In the current model, the adjusted maximum sedimentation rate was  $0.247 \text{ kg m}^{-2} \text{ day}^{-1}$  at  $x = 45 \text{ km}$  (keeping the local erosion rate at  $0.17 \text{ kg m}^{-2} \text{ day}^{-1}$ ), and the maximum erosion rate was  $0.251 \text{ kg m}^{-2} \text{ day}^{-1}$  at  $x = 60 \text{ km}$  (keeping the local sedimentation rate at  $0.17 \text{ kg m}^{-2} \text{ day}^{-1}$ ).

In the Scheldt campaigns of 1999 and 2000, the field data for SPM showed a turbidity cloud (relatively high SPM concentration) of respectively  $27$  and  $35 \text{ mg L}^{-1}$  around Hansweert ( $x = 55 \text{ km}$ ). In the campaign of 2000 only, a second SPM maximum ( $127 \text{ mg L}^{-1}$ ) situated near Antwerp (at the location where the salinity starts to increase,  $x = 15 \text{ km}$ ) was observed. The

maximum near Antwerp is considered a “classical” maximum turbidity zone occurring because the advection and dispersion of SPM are in equilibrium in that region, while the other SPM maximum occurs due to local net resuspension (Van Maldegem et al., 1993).

The SPM boundary concentrations in the model were fixed at the values of the actual samples. Consequently, the SPM concentration for the campaign of 1999 at  $x = 0$  km was set low ( $10 \text{ mg L}^{-1}$ ), resulting in only one SPM maximum at  $x = 55$  km, the one near Antwerp being absent. Results for the calculated and actual SPM concentrations at the 1999 and 2000 sampling days are shown in Fig. 6. Due to the increased sedimentation rate near Saeftinge and the increased erosion further downstream used in the model, the resulting calculated SPM maximum is not situated at the location where the velocity of SPM ( $U_{x,\text{spm}}$ ) is 0 ( $x = 20$  km) but more downstream ( $x = 55$  km).

For the Rhine estuary, an exchange of SPM between the surface and bottom water layer was incorporated, and exchange of SPM between water and sediment was only possible for the bottom layer. For lack of detailed data on sedimentation rates in the Rhine estuary, the SPM exchange rates between both the surface and bottom water layer and the bottom water layer and sediment were taken to be equal to the default exchange rates of SPM between sediment and water in the Scheldt estuary ( $0.17 \text{ kg m}^{-2} \text{ day}^{-1}$ ).

### 3.1.3. Biodegradation

After the salinity profile had been modeled accordingly, biodegradation processes were optimized. The reason to optimize biodegradation before the sorption processes was that the field data suggested biodegradation to be the main environmental process in the estuary (Jonkers et al., 2003). Sorption was neglected in this procedure.

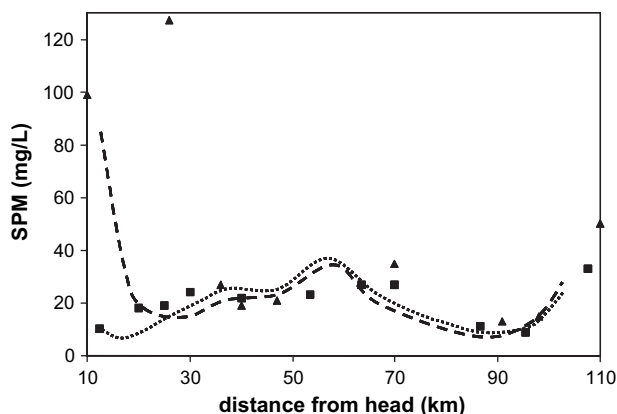


Fig. 6. Calculated and actual suspended particulate material concentrations in the Scheldt estuary at the two sampling times. ■, actual SPM concentration 1999; dotted line, calculated SPM concentration 1999; ▲, actual SPM concentration 2000; striped line, calculated SPM concentration 2000.

In the fate model, biodegradation is assumed to occur only in the dissolved phase. This assumption is supported by the findings of Shang et al. (1999), who observed an extremely slow degradation of  $A_9\text{PEO}$  in marine sediments, with estimated half-lives of more than 60 years. The oxidative hydrolytic pathway is assumed to be followed, resulting in the following modeled degradation routes:  $A_9\text{PEO}_{>2} \rightarrow A_9\text{PE}_{>2}\text{C} \rightarrow A_9\text{PE}_{1,2}\text{C} \rightarrow \text{X}$ ;  $A_9\text{PEO}_{1,2} \rightarrow A_9\text{PE}_{1,2}\text{C} \rightarrow \text{X}$ ; and  $\text{NP} \rightarrow \text{X}$  (X signifies subsequent metabolites, e.g. CAPEC, see Fig. 1 (Jonkers et al., 2001)).

Biodegradation rates were adjusted to optimize the fits of the calculated dissolved concentration profiles of  $A_9\text{PEO}$  and metabolites to the actual profiles. The optimization of the biodegradation rates for  $A_9\text{PEO}_{>2}$ ,  $A_9\text{PEO}_{1,2}$ , NP,  $A_9\text{PE}_{>2}\text{C}$  and  $A_9\text{PE}_{1,2}\text{C}$  was performed for the Scheldt data of the 1999 and 2000 sampling campaigns separately. Evidently, the rates for  $A_9\text{PEO}$  must be fitted before  $A_9\text{PEC}$ , as the degradation of the surfactant results in formation of  $A_9\text{PEC}$ , and therefore influences the fit of the subsequent degradation of  $A_9\text{PEC}$ . The optimum biodegradation rates are shown in Table 1.

In addition to the optimum values for biodegradation rates, validity intervals for this parameter were defined, based on the reliability of the analytical method for the field samples. After running the model with an adjusted biodegradation rate, for each model segment the percentual deviation between the concentration calculated with the new scenario and that of the optimum scenario was determined. These values were averaged, and compared to the relative standard deviation of the recovery of the analytical method (14, 5 and 13% for  $A_9\text{PEO}$ ,  $A_9\text{PEC}$  and NP, respectively (Jonkers et al., 2003)). When the former value is lower than the latter, the biodegradation rate lies within the validity interval.

Table 1

Process constants with validity intervals for the optimum model scenarios of the Scheldt estuary

	1999 data	2000 data
<i>Biodegradation rate constant (<math>\text{day}^{-1}</math>)</i>		
$A_9\text{PEO}_{>2}$	0.061 (0.049–0.077)	0.000 (0–0.007)
$A_9\text{PEO}_{1,2}$	0.070 (0.060–0.085)	0.057 (0.047–0.072)
$A_9\text{PE}_{>2}\text{C}$	0.017 (0.015–0.019)	0.030 (0.028–0.033)
$A_9\text{PE}_{1,2}\text{C}$	0.018 (0.016–0.020)	0.049 (0.046–0.053)
NP	0.032 <sup>a</sup> (0.024–0.043)	0.056 <sup>a</sup> (0.046–0.070)
<i>Sorption coefficient <math>K_d</math> (<math>\text{L kg}^{-1}</math>)</i>		
$A_9\text{PEO}_{>2}$	47000 (18800–89300)	47000 (31500–70500)
$A_9\text{PEO}_{1,2}$	33700 (10110–67400)	33700 (0–84300)
$A_9\text{PE}_{>2}\text{C}$	645 (0–5160)	645 (0–10320)
$A_9\text{PE}_{1,2}\text{C}$	645 (0–4580)	645 (0–13545)
NP	24900 (7221–52290)	24900 (0–72210)

<sup>a</sup> This rate includes the possible disappearance by volatilization. For the relatively volatile NP (compared to  $A_9\text{PEO}$ ), this process may be of significance.

As an example, when a biodegradation rate of 0.049 is chosen for  $A_9\text{PEO}_{>2}$  (1999 data, see Table 1), the concentrations of the dissolved profile calculated are higher than those obtained with the optimum biodegradation rate (0.061). When for each segment in the estuary the concentrations are compared with the optimum profile, the differences in concentrations are on average 14%. This value is equal to the relative standard deviation of the recovery of the analytical method for this compound, and therefore this biodegradation rate is defined to be the minimum value of the validity interval.

For  $A_9\text{PEO}$ , the half-life corresponding to the optimum biodegradation rate is 10–11 days (1999 data), which lies within the range of values reported in literature (ranging from 1.9 to 69 days (Ahel et al., 1994; Kveřtak and Ahel, 1995; Potter et al., 1999)).

No metabolites of NP were analyzed in the field studies, and therefore, the biodegradation rates are slightly less reliable than those of  $A_9\text{PEO}$ . Due to the relative volatility of NP (compared to  $A_9\text{PEO}$ ), a portion of the disappearance of NP from the water column may have been caused by volatilization instead of degradation.

For all compounds, photolysis may also play a role in their environmental fate, as these compounds have a tendency to accumulate at the water surface. This process was not considered separately and, if occurring, is incorporated in the biodegradation constant.

For  $A_9\text{PEC}$  and NP, biodegradation rates were smaller during the 1999 campaign, which was performed in winter. Biodegradation rates of  $A_9\text{PEO}_{1,2}$  were not significantly different for the two campaigns, while biodegradation of  $A_9\text{PEO}_{>2}$  proceeded more slowly in summer than in winter. At this point, no explanation can be given for the slower degradation rate of  $A_9\text{PEO}_{>2}$  in summer than in winter. Oxygen concentrations did not deviate significantly between the two sampling campaigns (both measured at 1.5 m depth).

For the Rhine estuary model, the same biodegradation rates as optimized for the Scheldt campaign of 1999 were employed.

#### 3.1.4. Sorption

After the biodegradation rates of all analytes had been fitted, sorption was introduced into the model. Average distribution coefficients between SPM and water (sorption coefficients,  $K_d$ ) of the analytes were used as calculated from the analyses of the water and SPM samples of both estuaries. The calculated  $K_d$  values were in agreement with other literature data (Ferguson et al., 2001; Heemken et al., 2001). As no salinity dependence of the  $K_d$  was observed for the field data, no salting out effects were incorporated into the model. Although in most SPM samples  $A_9\text{PEC}$  concentrations were below detection limits, sorption was incorporated in the model for these compounds, with a  $K_d$  value based on the few

SPM samples in which  $A_9\text{PEC}$  were detected (Jonkers et al., 2003).

Resulting analyte concentrations in SPM and sediment as calculated by the model were of the same order of magnitude as the field data, and therefore no further optimization of sorption coefficients was performed. Again, validity intervals with minimum and maximum sorption coefficients were determined as described in Section 3.1.3 (see Table 1).

After the introduction of sorption into the model, the biodegradation rates were again slightly adjusted, as the sorption processes will have some influence on the fit. Degradation rates had to be slightly increased, as the analytes sorbed to the SPM are “shielded” from degradation.

#### 3.1.5. Additional sources

To obtain acceptable model fits of the concentration profiles in the Rhine estuary, it was necessary to incorporate two additional point sources. These were the Oude Maas tributary ( $x = 18$  km) and a source in the Rotterdam harbor area ( $x = 12$  km). Input concentrations were fitted to the concentration profiles in the estuary, as the actual analyte concentrations were unknown for these sources. The values are shown in Table 2 (see also Section 3.2.5). A recent report on the analysis of  $A_9\text{PEO}$  in rainwater of this region confirms the presence of these suspected sources (Peters, 2003).

For the additional water source in the Scheldt estuary (canal Gent–Terneuzen,  $x = 81$  km), initially the actual  $A_9\text{PEO}$ ,  $A_9\text{PEC}$  and NP concentrations were fixed in the model. As a final optimization step, these values were also fitted to the observed concentration profiles in the estuary, and the adjusted concentrations used in the optimum scenario are shown in Table 2 (2–10 times the actual concentrations in the canal for the different analytes).

### 3.2. Comparison to field results

A short description of the results of the several sampling campaigns will be given, followed by the comparison of model results and field data. The results of the sampling campaigns of 1999 (Section 3.2.1) were reported previously by Jonkers et al. (2003). For all sampling campaigns, the observed concentrations are within the ranges reported in literature for estuarine or waters (0.005–25  $\mu\text{g L}^{-1}$  and <0.02–5.8  $\mu\text{g L}^{-1}$  for  $A_9\text{PEO}$  and NP, respectively) and sediments (<0.002–4.0  $\mu\text{g g}^{-1}$  dry weight and <0.002–9.0  $\mu\text{g g}^{-1}$  dry weight for  $A_9\text{PEO}$  and NP, respectively) (Jonkers and De Voogt, 2003).

#### 3.2.1. Sampling campaigns of 1999

The dissolved concentration profiles in the Scheldt estuary showed a stronger than conservative decrease in

Table 2

Final input values of dissolved concentrations and loads of the sources used in the optimum model scenarios for the Scheldt estuary (1999) and Rhine estuary (2002)

Source	Compound				
	A <sub>9</sub> PEO <sub>&gt;2</sub>	A <sub>9</sub> PEO <sub>1,2</sub>	A <sub>9</sub> PE <sub>&gt;2</sub> C	A <sub>9</sub> PE <sub>1,2</sub> C	NP
<i>Scheldt estuary</i>					
Canal Gent–Terneuzen (ng L <sup>-1</sup> )	1540	500	3350	9460	640
Total input canal Gent–Terneuzen (kg day <sup>-1</sup> )	2.3	0.73	4.9	13.9	0.93
Total input at head of estuary (kg day <sup>-1</sup> )	11.4	9.3	14.7	83.0	8.4
<i>Rhine estuary</i>					
Oude Maas surface layer (ng L <sup>-1</sup> )	0	0	0	125	56
Oude Maas bottom layer (ng L <sup>-1</sup> )	0	0	125	525	20
Total input Oude Maas (kg day <sup>-1</sup> )	0	0	7.6	39.3	4.6
Harbor surface layer (ng L <sup>-1</sup> )	4000	800	7700	10000	2000
Harbor bottom layer (ng L <sup>-1</sup> )	5500	700	2800	8000	1300
Total input harbor (kg day <sup>-1</sup> )	8.2	1.3	9.1	15.6	2.9
Total input at head of estuary (kg day <sup>-1</sup> )	8.0	2.3	16.5	46.8	14.0

A<sub>9</sub>PEO from Antwerp to Vlissingen, while the A<sub>9</sub>PEC metabolites concentration decreased more slowly. The  $\Sigma A_9PEC/\Sigma A_9PEO$  concentration ratio therefore increased going downstream, suggesting the formation of A<sub>9</sub>PEC out of A<sub>9</sub>PEO in the estuary. The dissolved A<sub>9</sub>PEC/A<sub>9</sub>PEO ratio reached a maximum near Terneuzen, followed by a decrease further downstream. The water inside canal Gent–Terneuzen showed a high A<sub>9</sub>PEC/A<sub>9</sub>PEO ratio as well.

For the Rhine estuary, the profiles of the water concentrations appeared to be less pronounced, probably due to more complicated water flows and point sources in the Rotterdam harbor area. Dissolved A<sub>9</sub>PEC/A<sub>9</sub>PEO ratios were fairly constant with values between 2 and 3. These findings indicate that biodegradation is only limited in this estuary, which is not surprising because of the high water flow and short residence time. Maximum dissolved estuarine concentrations amounted to 1.3, 1.0, 0.9 and 8.1  $\mu\text{g L}^{-1}$  for A<sub>9</sub>PEO<sub>>2</sub>, A<sub>9</sub>PEO<sub>1,2</sub>, NP and  $\Sigma A_9PEC$ , respectively.

In sediments, concentrations normalized to the fraction with particle sizes < 63  $\mu\text{m}$  showed a maximum of 4500 (A<sub>9</sub>PEO<sub>>2</sub>), 998 (A<sub>9</sub>PEO<sub>1,2</sub>) and 2600 (NP)  $\text{ng g}^{-1}$ , whereas A<sub>9</sub>PEC were only present sporadically. No gradients were observed for the sediment concentrations. Concentrations in estuarine SPM varied strongly from 690 to 115,000  $\text{ng g}^{-1}$  for A<sub>9</sub>PEO and from 190 to 30,400  $\text{ng g}^{-1}$  for NP.

### 3.2.2. Sampling campaign of 2000

The concentrations of A<sub>9</sub>PEO, NP and A<sub>9</sub>PEC observed in the sampling campaign of 2000 are listed in Tables 3 and 4. In general, dissolved concentrations were about half of those observed in the first sampling campaigns. The highest dissolved concentrations of A<sub>9</sub>PEO were observed near Antwerp, with values of 450  $\text{ng L}^{-1}$  for A<sub>9</sub>PEO<sub>>2</sub> and 680  $\text{ng L}^{-1}$  for A<sub>9</sub>PEO<sub>1,2</sub>. In the Rhine estuary, dissolved A<sub>9</sub>PEO concentrations were invariably below 250  $\text{ng L}^{-1}$ . The concentrations of

NP observed in water were mostly below the level of 100  $\text{ng L}^{-1}$ . Only in the upper Scheldt estuary, dissolved concentrations of NP were higher, with a maximum of 960  $\text{ng L}^{-1}$  near Antwerp. The highest dissolved estuarine  $\Sigma A_9PEC$  concentrations were found near Antwerp as well. An overall maximum value of 6500  $\text{ng L}^{-1}$  was observed inside the canal Gent–Terneuzen.

In the Scheldt estuary, the dissolved concentration gradients along salinity reported for the campaign of 1999 could be observed again, with a faster than conservative decrease of both A<sub>9</sub>PEO and metabolite concentrations. However, the decrease of A<sub>9</sub>PEO was less steep than in the first campaign. Dissolved  $\Sigma A_9PEC/\Sigma A_9PEO$  ratios varied between 1.3 and 6.9, and did not show a clear maximum as observed during the 1999 campaign.

In the Rhine estuary, dissolved A<sub>9</sub>PEC/A<sub>9</sub>PEO ratios were determined between 0.3 and 5.4. Dissolved NP/A<sub>9</sub>PEO ratios varied in both estuaries between 0.05 and 1.8. No clear spatial trends could be observed.

Normalizing the surface sediment data to the fraction < 63  $\mu\text{m}$  resulted in maximum concentrations of 4000 (A<sub>9</sub>PEO<sub>>2</sub>, location R8s), 1200 (A<sub>9</sub>PEO<sub>1,2</sub>, R8s) and 2000  $\text{ng g}^{-1}$  (NP, S9s). Concentrations were in the same range as in the campaigns of 1999. A<sub>9</sub>PEC were detected in half the number of sediments collected, at a maximum normalized concentration of 3200  $\text{ng g}^{-1}$ . No spatial trends were observed for concentrations in sediment.

The median contributions of the analytes sorbed onto SPM to the total water concentrations (dissolved + sorbed) calculated for both estuaries amounted to 35, 20, 37 and 16% for A<sub>9</sub>PEO<sub>>2</sub>, A<sub>9</sub>PEO<sub>1,2</sub>, NP and A<sub>9</sub>PEC, respectively. For this calculation, only those samples were used for which both phases had concentrations above detection limits.

$K_{oc}$  values were calculated for A<sub>9</sub>PEO and NP. For both analytes values were found to vary between  $\log K_{oc} = 4.2$  and 7.1. Average  $\log K_{oc}$  values ( $\pm$  standard

Table 3

Concentrations of A<sub>9</sub>PEO and their metabolites measured in surface sediment and suspended particulate material in the Rhine and Scheldt estuary, 2000

Sample name	Organic carbon (%)	Fraction <63 μm	A <sub>9</sub> PEO <sub>1</sub> (ng/g d.w.)	A <sub>9</sub> PEO <sub>2</sub> (ng/g d.w.)	A <sub>9</sub> PEO <sub>&gt;2</sub> (ng/g d.w.)	NP (ng/g d.w.)	A <sub>9</sub> PE <sub>1,2</sub> C total (ng/g d.w.)	A <sub>9</sub> PE <sub>&gt;2</sub> C (ng/g d.w.)
<i>Rhine sediments, 2000</i>								
R1s	0.15	0.048	<1.3	0.3	3.9	7.1	<0.4	<0.3
R2s	0.17	0.036	<1.3	1.3	20	14	<0.4	<0.3
R3s	0.06	0.005	<1.3	1.4	14	3.9	6.3	<0.3
R4s	1.5	0.35	8.7	16	121	124	<0.4	<0.3
R5s	0.46	0.32	3.7	3.6	22	54	<0.4	<0.3
R6s	2.3	0.50	19	25	123	223	<0.4	<0.3
R7s	0.09	0.012	<1.3	1.2	26	16	15	8.2
R8s	0.11	0.004	3.5	1.4	16	5.7	8.6	2.5
<i>Scheldt sediments, 2000</i>								
S1s	0.2	0.028	<1.3	1.4	19	11	2.1	<0.3
S2s	0.18	0.024	<1.3	0.6	13	3.7	<0.4	<0.3
S3s	0.06	0.009	<1.3	<0.3	2.0	3.6	<0.4	<0.3
S4s	2.1	0.59	33	34	554	1014	54	<0.3
S5s	0.07	0.007	<1.3	0.8	10	3.2	15	6.8
S6s	<0.05	0.009	<1.3	1.0	7.1	6.9	3.3	2.7
S7s	0.2	0.045	<1.3	1.5	11	44	0.7	<0.3
S8s	0.09	0.008	4.5	1.6	24	–	–	–
S9s	2.9	0.52	36	32	332	1057	<0.4	<0.3
S10s	7.8	0.44	5.3	10	49	375	70	<0.3
SCs	1.4	0.41	32	38	293	1026	172	560
<i>Rhine SPM, 2000</i>								
R11f	1.3		<88	264	1576	437	<24	<18
R12f	5.5		<88	<19	5205	2319	<24	<18
R13f	5.3		<88	831	4840	2158	<24	<18
R14f	5.0		<88	776	4227	1993	<24	<18
R15f	5.8		<88	960	4548	1387	<24	<18
R16f	5.3		<88	566	13605	6105	<24	<18
R17f	5.0		<88	78	7616	1550	<24	<18
R18f	4.2		513	97	1965	1230	<24	<18
<i>Scheldt SPM, 2000</i>								
S11f	10.8		2344	177	2808	11025	<24	<18
S12f	2.8		196	26	509	8694	<24	<18
S13f	4.6		<88	66	1022	5943	<24	<18
S14f	5.7		1270	309	2752	1856	<24	<18
S15f	4.0		<88	154	2294	764	<24	<18
S16f	4.8		<88	305	1641	1052	<24	<18
S17f	5.7		<88	313	4279	2553	<24	<18
S18f	6.3		<88	319	5977	2464	<24	<18
S19f	5.9		191	194	1208	1762	1812	3020
S20f	4.3		386	225	1059	1233	702	1435
S21f	–		448	280	1093	1651	1424	1954
S22f	7.6		1171	731	2028	2480	6986	8416
SCf	25.7		1231	3784	8176	16637	6056	7534

deviations) were  $5.8 \pm 0.5$  (A<sub>9</sub>PEO<sub>>2</sub>),  $5.5 \pm 0.7$  (A<sub>9</sub>PEO<sub>1,2</sub>) and  $6.0 \pm 0.5$  (NP). For the five SPM samples in which A<sub>9</sub>PEC were detected, a log  $K_{oc}$  was calculated of  $4.5 \pm 0.3$ .

### 3.2.3. Sampling campaign of 2002

Table 5 shows the analytical results for the 2002 water sampling campaign in the Rhine estuary. At locations R21 to R24, the salinity values illustrate the vertical stratification of the water column. At the locations upstream, salinities were close to 0 both at the surface and at greater depth.

Maximum concentrations amounted to 300 (A<sub>9</sub>PEO<sub>>2</sub>), 70 (A<sub>9</sub>PEO<sub>1,2</sub>), 160 (NP) and 940 ng L<sup>-1</sup> (ΣA<sub>9</sub>PEC). A<sub>9</sub>PEC were usually present at higher concentrations than A<sub>9</sub>PEO, with a median dissolved ΣA<sub>9</sub>PEC/ΣA<sub>9</sub>PEO concentration ratio of 7.3.

At all sampling locations except one (location R27), A<sub>9</sub>PEO concentrations were higher in the water samples taken from the surface than those taken at greater depth. This vertical stratification of A<sub>9</sub>PEO was present both in the saline part of the estuary and in the part where the complete water column consists of freshwater. The stratification did increase at higher salinities, with

Table 4

Dissolved concentrations of A<sub>9</sub>PEO and their metabolites measured in the Rhine and Scheldt estuary, 2000

Sample name	Salinity (‰)	Temperature (°C)	Oxygen concentration (mg L <sup>-1</sup> )	SPM (mg L <sup>-1</sup> )	A <sub>9</sub> PEO <sub>1</sub> (ng L <sup>-1</sup> )	A <sub>9</sub> PEO <sub>2</sub> (ng L <sup>-1</sup> )	A <sub>9</sub> PEO <sub>3–15</sub> (ng L <sup>-1</sup> )	NP (ng L <sup>-1</sup> )	A <sub>9</sub> PE <sub>1</sub> C (ng L <sup>-1</sup> )	A <sub>9</sub> PE <sub>2</sub> C (ng L <sup>-1</sup> )	A <sub>9</sub> PE <sub>&gt;2</sub> C (ng L <sup>-1</sup> )
<i>Rhine estuary</i>											
R11w	29.0	17.7	7.6	20	<15	<6	<30	15	64	<13	<13
R12w	19.0	19.1	8.2	6	<15	8.4	36	13	110	75	39
R13w	14.0	19.9	8.2	6	<15	7.9	185	18	60	<13	<13
R14w	11.5	20.3	8.0	6	<15	11	225	38	83	40	<13
R15w	7.5	17.9	8.6	6	<15	23	66	88	188	116	115
R16w	5.3	18.1	9.2	6	<15	9.5	62	38	177	144	86
R17w	2.9	18.1	9.3	7	<15	23	68	48	77	<13	<13
R18w	1.0	18.3	9.1	26	<15	12	196	12	109	<13	<13
<i>Scheldt estuary</i>											
S11w	32.6	17.0	7.8	4	<15	6.8	<30	50	37	<13	<13
S12w	30	18.3	8.4	50	<15	29	42	62	82	47	15
S13w	27.5	18.7	8.1	15	<15	8.4	34	58	49	<13	13
S14w	23.8	19.2	7.8	13	<15	9.9	55	28	77	66	50
S15w	21.1	19.5	7.9	35	19	16	144	55	329	488	432
S16w	17.9	19.9	8.0	27	18	43	175	81	150	212	122
S17w	15.2	20.1	7.2	21	22	27	55	92	200	267	153
S18w	11.9	20.5	6.5	19	56	73	193	105	321	499	388
S19w	9.0	20.9	5.5	27	81	88	195	184	359	691	530
S20w	6.0	21.6	3.2	127	49	48	111	282	360	598	485
S21w	2.4	–	–	–	145	99	186	394	905	1163	561
S22w	0.53	22.5	0.33	99	443	234	447	962	644	1042	506
SCw	4.3	23.0	5.1	3	73	200	543	272	1030	2339	3123

dissolved ratios of A<sub>9</sub>PEO<sub>surface</sub>/A<sub>9</sub>PEO<sub>max.depth</sub> increasing from 1.5 at a bottom water salinity of 0.16 to 3.9 at a bottom water salinity of 28. Apparently, the vertical stratification of A<sub>9</sub>PEO in the water column is not only caused by the stratification of the water, but also because of the surface active properties of A<sub>9</sub>PEO itself. For the metabolites A<sub>9</sub>PEC and NP, a vertical stratification is only observed at the saline end of the estuary. Concentration ratios of A<sub>9</sub>PEC<sub>surface</sub>/A<sub>9</sub>PEC<sub>max.depth</sub> and NP<sub>surface</sub>/NP<sub>max.depth</sub> are around one at most locations, and increase at locations R21 to R24 to 2.2 (A<sub>9</sub>PEC) and 4.3 (NP). The fact that these compounds are hardly surface active explains the absence of a stratification in the freshwater part of the estuary.

The lowest dissolved A<sub>9</sub>PEO concentrations in the Rhine estuary were found at both the river and the sea end boundaries of the estuaries (at all sampling depths). Maximum concentrations were observed around the harbors of Rotterdam. Apparently, local sources such as the harbors or the river Oude Maas play a more important role in the distribution of A<sub>9</sub>PEO in the estuary than the input from the Rhine and the North Sea. For NP and A<sub>9</sub>PEC, concentrations were lowest at the sea end of the estuary, and fairly evenly distributed in the rest of the area.

### 3.2.4. Validation procedure

As mentioned above, the analytical results yielded smooth spatial concentration profiles for the dissolved

analytes in most sampling campaigns (Jonkers et al., 2003). Therefore, it was possible to interpolate the data points, and obtain a curve of concentration vs. distance which could be directly compared to the output curves of the model. In this way, the quality of the fit could be determined by calculating the percentual deviations between the points of the model curve and those of the curve of the actual data. The average of these (absolute) values will be referred to as the quality of the fit (with a decrease in this number signifying an increase in quality of the fit). Results of this procedure are listed in Table 6 for different model scenarios (see Section 3.2.5 and further). This table facilitates a quantitative comparison of the model scenarios.

To determine the significance of the deviation between two calculated concentration profiles, a method was used similar to the determination of the validity intervals of the process constants (see Section 3.1.4). Two profiles are considered to deviate significantly from each other when the average percentual deviation between the concentrations of the two profiles is higher than the standard deviation of the recovery of the analytical method.

For the A<sub>9</sub>PEO and metabolites concentrations in SPM and sediment, smooth curves could not be constructed, as no clear spatial trends were present. Therefore, only a general quality of the fit could be determined by checking if the calculated curve passed through the middle of the scatter of field data points.

Table 5  
Dissolved concentrations of A<sub>9</sub>PEO and metabolites measured in the Rhine estuary at different sampling depths, 2002

Sample name	Salinity (‰)	SPM (mg L <sup>-1</sup> )	A <sub>9</sub> PEO <sub>1</sub> (ng L <sup>-1</sup> )	A <sub>9</sub> PEO <sub>2</sub> (ng L <sup>-1</sup> )	A <sub>9</sub> PEO <sub>&gt;2</sub> (ng L <sup>-1</sup> )	NP (ng L <sup>-1</sup> )	A <sub>9</sub> PE <sub>1</sub> C (ng L <sup>-1</sup> )	A <sub>9</sub> PE <sub>2</sub> C (ng L <sup>-1</sup> )	A <sub>9</sub> PE <sub>&gt;2</sub> C (ng L <sup>-1</sup> )
<i>Water Rhine estuary surface</i>									
R21w1	15.9	8	<15	<6	48	38	184	92	132
R22w1	11.6	14	<15	9.4	108	58	219	116	167
R23w1	8.8	13	<15	7.4	82	80	256	143	185
R24w1	6.0	13	<15	16	84	34	293	194	248
R25w1	4.4	14	15	8.4	95	115	229	139	142
R26w1	0.37	26	<15	64	299	67	283	170	187
R27w1	0.25	28	<15	<6	42	102	263	143	172
R28w1	0.32	16	24	17	126	66	284	175	174
R29w1	0.26	18	21	28	203	134	367	247	327
R30w1	0.18	20	32	8.2	95	113	264	143	178
R31w1	0.16	20	22	13	136	136	192	92	101
R32w1	0.16	22	<15	7.1	59	123	278	181	183
R33w1	0.16	28	<15	9.8	74	82	220	138	139
<i>Water Rhine estuary 1.5 m depth</i>									
R21w2	23.3	8	<15	<6	38	30	90	53	45
R22w2	12.2	18	<15	<6	40	40	224	131	136
R23w2	9.0	15	<15	6.0	38	48	265	170	179
R24w2	6.8	15	<15	<6	33	100	225	145	131
R25w2	4.6	16	<15	9.1	43	92	225	125	110
R26w2	0.50	35	<15	13	70	77	284	194	184
R27w2	0.70	61	<15	13	66	94	201	100	73
R28w2	0.30	18	<15	16	70	80	261	169	188
R29w2	0.30	22	21	40	178	105	316	203	193
R30w2	0.20	22	<15	11	51	78	255	156	132
R31w2	0.16	24	<15	6.8	42	162	330	216	202
R32w2	0.16	29	<15	9.8	47	93	200	125	99
R33w2	0.16	29	<15	6.3	43	152	285	202	203
<i>Water Rhine estuary maximum depth</i>									
R21w3	28.5	7	<15	<6	<30	17	61	27	<13
R22w3	23.6	13	<15	<6	<30	28	104	63	42
R23w3	11.2	15	<15	9.4	51	37	226	154	176
R24w3	10.6	15	<15	7.1	40	36	213	130	141
R25w3	4.7	18	<15	7.7	54	148	256	169	144
R26w3	0.86	36	<15	12	54	59	273	194	209
R28w3	0.36	27	<15	12	85	130	322	193	208
R31w3	0.16	25	<15	14	76	123	211	124	106
R32w3	0.16	28	<15	7.1	39	75	316	213	223
R33w3	0.16	33	<15	11	42	121	197	122	99

The calculated sediment concentrations were compared to the analyzed sediment concentrations normalized to the particle size fraction <63 µm, as it was assumed that this is the sediment fraction which has actual exchange with the SPM.

### 3.2.5. Calculated concentration profiles

For the Scheldt estuary, the model runs were started at January 1, 1999. Concentration profiles for the day of sampling (November 17, 1999, day 321) were calculated in the optimum scenario as shown in Fig. 7a–d. Satisfactory fits of the dissolved concentration profiles were obtained. The quality of the fits of the optimum scenario are given in Table 6, model scenario I. For concentrations in SPM and sediment, deviations between the model and actual data were larger, but calculated and actual concentrations were of the same

order of magnitude. This was considered the best possible result with the current model type.

For the additional source canal Gent–Terneuzen, the total input amounted to 8–33% of the input at the head of the estuary for the different compounds (see Table 2).

For the Scheldt data of 2000 (June 20, 2000, day 536 in the model), calculated and actual concentration profiles are shown in Fig. 8a–d and Table 6 (scenario XIII).

The fate model for the Rhine estuary was compared to the results of the 2002 sampling campaign, in which samples at different depths were taken. In this comparison, only the analytical results of the samples taken at the water surface and those taken at maximal depths were considered. Initially, the fits were not entirely satisfactory (Table 6, scenario XV), as the actual concentration “humps” in the middle of the estuary could not be modeled without additional A<sub>9</sub>PEO sources in the

Table 6  
Quality of fit of the calculated dissolved concentration profiles for the different model scenarios

Model scenario		Average (absolute value of) percentual deviation from actual values				
		NP	A <sub>9</sub> PEO <sub>&gt;2</sub>	A <sub>9</sub> PEO <sub>1,2</sub>	A <sub>9</sub> PE <sub>&gt;2</sub> C	A <sub>9</sub> PE <sub>1,2</sub> C
<i>Scheldt 1999</i>						
<b>I</b>	<b>Optimum scenario</b>	<b>26</b>	<b>29</b>	<b>23</b>	<b>12</b>	<b>17</b>
II	Dispersion coefficients 100 m <sup>2</sup> s <sup>-1</sup>	42	52	47	17	26
III	Dispersion coefficients 200 m <sup>2</sup> s <sup>-1</sup>	34	44	37	12	22
IV	Dispersion coefficients 300 m <sup>2</sup> s <sup>-1</sup>	33	46	41	13	21
V	No sorption	39	48	35	14	18
VI	Sorption coefficients 5× optimum value	33	37	34	18	16
VII	Concentrations in canal Gent–Terneuzen zero	31	39	31	14	22
VIII	Concentrations in canal Gent–Terneuzen 3× optimum values	30	36	35	28	26
IX	No biodegradation	129	179	309	30	67
X	Biodegradation rates 0.5× optimum values	53	62	75	22	31
XI	Biodegradation rates 2× optimum values	32	36	37	24	25
XII	Salinity dependent biodegradation	21	19	21	13	16
<i>Scheldt 2000</i>						
<b>XIII</b>	<b>Optimum scenario</b>	<b>21</b>	<b>33</b>	<b>26</b>	<b>35</b>	<b>24</b>
<i>Rhine 2002</i>						
<b>XIV</b>	<b>Optimum scenario</b>	<b>22</b>	<b>20</b>	<b>28</b>	<b>19</b>	<b>13</b>
XV	Concentrations additional sources zero	34	51	42	47	43
XVI	No sorption	22	21	29	19	13
XVII	No biodegradation	22	23	31	19	13
XVIII	Biodegradation rates 5× optimum values	24	23	26	20	14

For each scenario, the difference with the corresponding optimum scenario is described. A smaller value indicates a better fit. For further explanation see Section 3.2.4.

estuary. As it is likely that the harbors of Rotterdam constitute additional sources of A<sub>9</sub>PEO, a point source was added into the model (De Beer et al., 1996). The location of this source was chosen to be at 12 km, which was suggested by the maxima in the observed concentration profiles. This source would correspond to the Eem Harbor of Rotterdam. Another likely additional source is the river Oude Maas, which discharges into the estuary at  $x = 18$  km. Optimized input concentrations for both sources are shown in Table 2. With these additional sources, satisfactory dissolved concentration profiles for the surface and bottom water layers were obtained with the optimum scenario, as shown in Fig. 9. The quality of the fits are listed in Table 6 (scenario XIV).

For some analytes, the inputs of these additional sources are relatively high. For the harbor, the inputs range from 20 to 100% of the input at the head of the estuary for the different analytes, and for the Oude Maas these values range from 0 to 84%. This illustrates the importance of additional discharges in this area.

With the analytical results of the water samples from the 1999 and 2000 campaigns in the Rhine estuary, it was more difficult to evaluate the fit of the fate model. Most of those water samples were taken along the salinity gradient, which intrudes only several kilometers into the estuary (see Fig. 2a). Therefore, for the major part of the estuary, no data on concentrations in water are available from those campaigns. However, when the model was applied to the concentration data in this

limited part of the estuary for the campaign of 2000, with the corresponding boundary concentrations and river discharge data, a satisfactory fit was obtained for the dissolved phase (water samples, taken at 1.5 m depth, were compared to the surface layer in the model, see Fig. 10a,b). The sediment and SPM data can be used to get an idea of the validity of the sorption coefficients and sedimentation/erosion rates that were used. As is shown in Fig. 10c,d, the calculated concentrations in SPM compare favorably with the field data, while the calculated concentrations in sediments were roughly an order of magnitude higher than the actual concentrations. This indicates that the sorption coefficients used in the model were correct, and that the exchange between SPM and sediment was overestimated for the Rhine estuary. Alternatively, degradation in the sediment could explain the relatively low actual concentrations in the sediments.

### 3.3. Sensitivity analysis

Several parameters in the optimum model scenarios were subjected to a sensitivity analysis. The influence of four parameters on the calculated concentration profiles was investigated: dispersion, sorption, additional sources and biodegradation.

For the Rhine estuary model, it was found that variation of both sorption and biodegradation had little influence on the dissolved concentration profiles. For

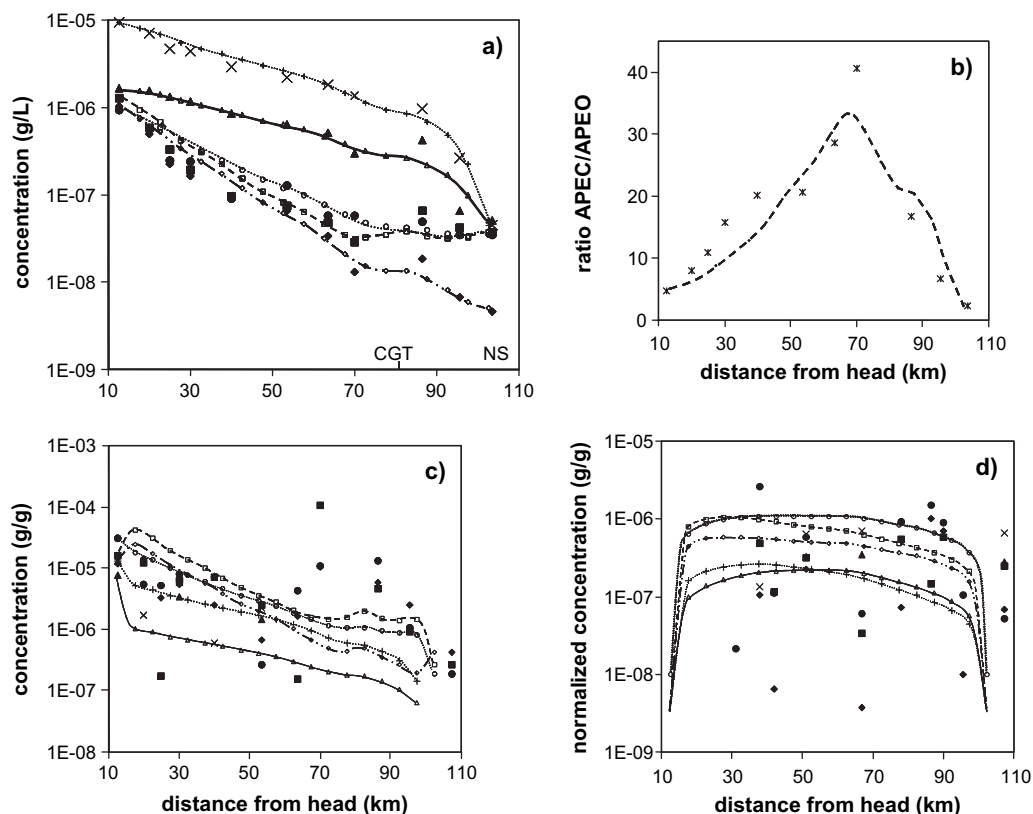


Fig. 7. Calculated and actual concentrations for the 1999 Scheldt data: (a) dissolved concentrations; (b) ratio of dissolved  $A_9$ PEC and  $A_9$ PEO; (c) concentrations in SPM; (d) concentrations in sediment.  $\times$ , actual  $A_9PE_{1,2}C$ ;  $+$  and dotted line, calculated profile;  $\blacktriangle$ , actual  $A_9PE_{>2}C$ ;  $\triangle$  and solid line, calculated profile;  $\bullet$ , actual NP;  $\circ$  and dotted line, calculated profile;  $\blacksquare$ , actual  $A_9PEO_{>2}$ ;  $\square$  and striped line, calculated profile;  $\blacklozenge$ , actual  $A_9PEO_{1,2}$ ;  $\diamond$  and striped/dotted line, calculated profile;  $*$ , actual  $A_9PEC/A_9PEO$  ratio; striped line, calculated ratio. CGT, position of canal Gent-Terneuzen; NS, North Sea side of the estuary.

example, when sorption is neglected in the model, the concentration profiles change only marginally, with average deviations from the optimum scenario from 0.03 to 1.5% for the different analytes (Table 6, scenario XVI). When the biodegradation rates were set to 0, the average deviations from the optimum scenario ranged from 0.7 to 6.3% for the different analytes (scenario XVII). When increasing the biodegradation rates, the increase must be as much as a factor 5 to obtain significant deviations (see Section 3.2.4) from the optimum curves (Table 6, scenario XVIII). A likely explanation of this limited influence of biodegradation and sorption on the fate of  $A_9$ PEO in the Rhine estuary is the relatively short residence time of  $A_9$ PEO in the Rhine estuary (several days, compared to 2–3 months for the Scheldt estuary). As already mentioned in Section 3.2.5, the parameter to which the model appeared to be the most sensitive was the insertion of additional  $A_9$ PEO sources. When this input was set to 0, a significant deviation from the optimum curve of 27–48% for the different analytes was calculated (Table 6, scenario XV).

The sensitivity analysis of the model for the Scheldt estuary of 1999 will be discussed in more detail in the following paragraphs.

### 3.3.1. Sensitivity towards dispersion coefficients

The implementation of different sets of dispersion coefficients in the Scheldt model of 1999 resulted in qualities of fit as shown in Table 6 (scenarios II–IV). Variation of the dispersion coefficients appeared to have some influence on the concentration profiles. However, when using dispersion coefficients of  $200 \text{ m}^2 \text{ s}^{-1}$  for each segment of the estuary (scenario III), the deviation of the calculated  $A_9$ PEO and NP profiles from the optimum scenario was not significant. For model scenarios with dispersion coefficients of  $100$  or  $300 \text{ m}^2 \text{ s}^{-1}$  for each segment (scenarios II and IV, respectively), the deviations from the optimum scenario became significant.

### 3.3.2. Sensitivity towards sorption

As Fig. 11a illustrates for  $A_9PEO_{>2}$ , relatively large changes in sorption coefficients were necessary in order to obtain significant deviations of the dissolved concentration profiles from the optimum scenarios. In other words, the concentration profiles were relatively insensitive towards sorption. This insensitivity is also illustrated with the sorption coefficient validity intervals in Table 1, which are large compared to those of the biodegradation rates.

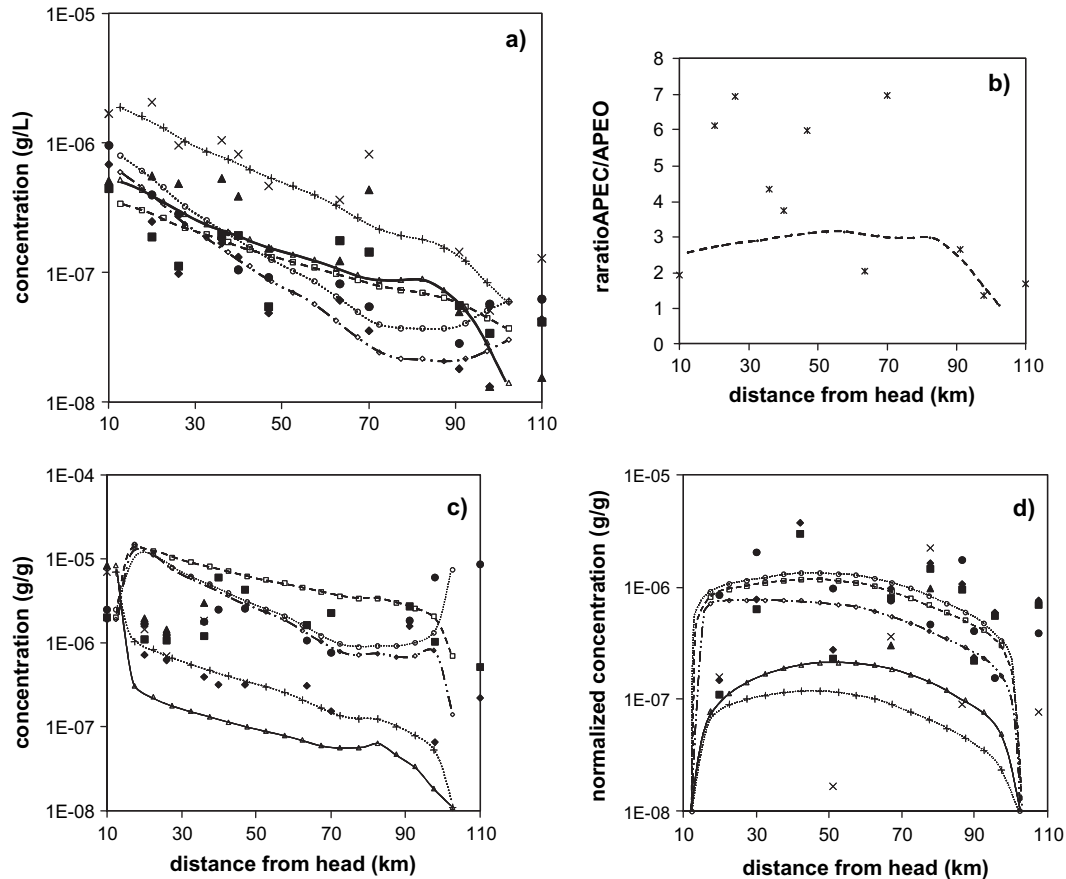


Fig. 8. Calculated and actual concentrations for the 2000 Scheldt data: (a) dissolved concentrations; (b) ratio of dissolved  $A_9$ PEC and  $A_9$ PEO; (c) concentrations in SPM; (d) concentrations in sediment.  $\times$ , actual  $A_9PE_{1,2}C$ ; + and dotted line, calculated profile;  $\blacktriangle$ , actual  $A_9PE_{>2}C$ ;  $\triangle$  and solid line, calculated profile;  $\bullet$ , actual NP;  $\circ$  and dotted line, calculated profile;  $\blacksquare$ , actual  $A_9PEO_{>2}$ ;  $\square$  and striped line, calculated profile;  $\blacklozenge$ , actual  $A_9PEO_{1,2}$ ;  $\diamond$  and striped/dotted line, calculated profile; \*, actual  $A_9PEC/A_9PEO$  ratio; striped line, calculated ratio.

As examples, the quality of the fits of concentration profiles for scenarios with the sorption coefficient set to 0 or to 5 times the optimum value are shown in Table 6 (scenarios V and VI, respectively).

### 3.3.3. Sensitivity towards an additional $A_9$ PEO source

As a high ratio of dissolved concentrations of  $A_9PEC/A_9PEO$  was observed in both the water of the canal Gent–Terneuzen and near its discharge point in

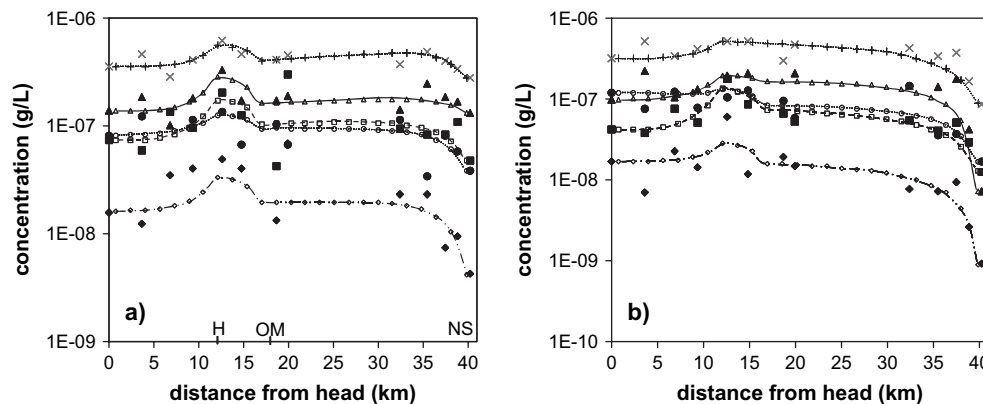


Fig. 9. Calculated and actual concentrations for the final 2002 Rhine data: (a) dissolved concentrations in the surface layer; (b) dissolved concentrations in the bottom layer.  $\times$ , actual  $A_9PE_{1,2}C$ ; + and dotted line, calculated profile;  $\blacktriangle$ , actual  $A_9PE_{>2}C$ ;  $\triangle$  and solid line, calculated profile;  $\bullet$ , actual NP;  $\circ$  and dotted line, calculated profile;  $\blacksquare$ , actual  $A_9PEO_{>2}$ ;  $\square$  and striped line, calculated profile;  $\blacklozenge$ , actual  $A_9PEO_{1,2}$ ;  $\diamond$  and striped/dotted line, calculated profile. H and OM, position of the additional sources: harbor and Oude Maas river; NS, North Sea side of the estuary.

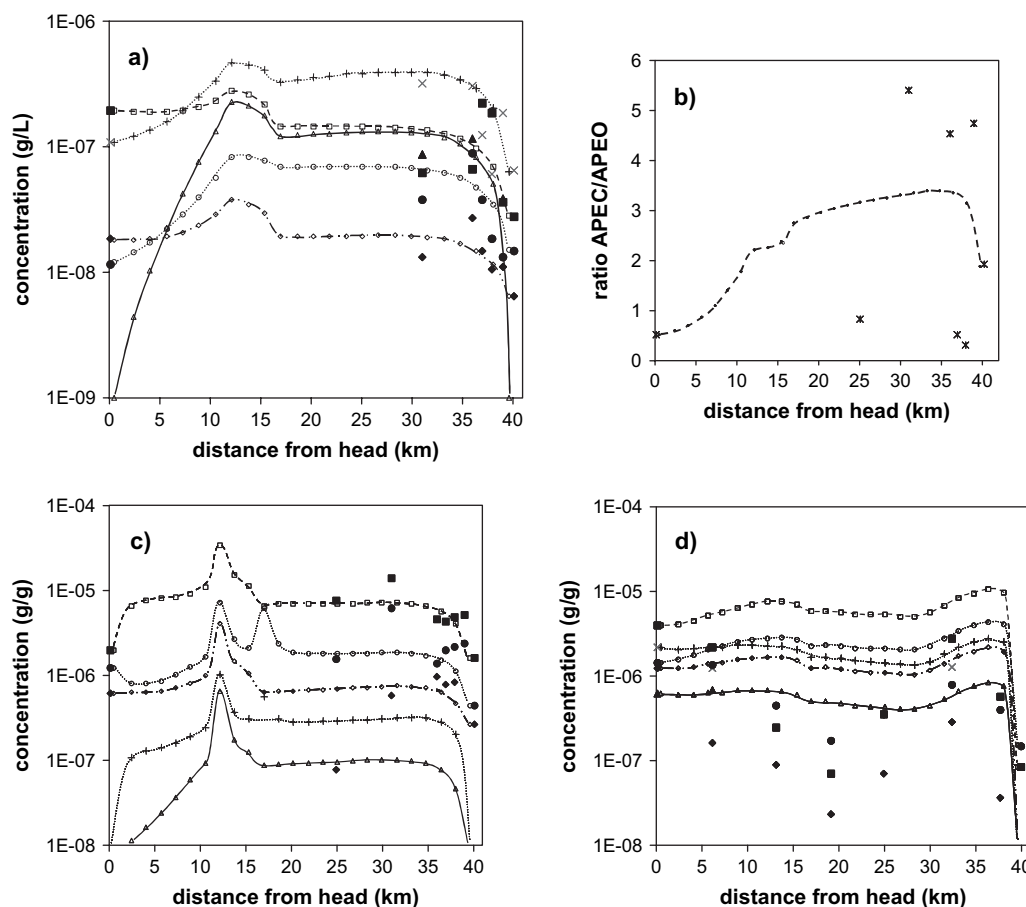


Fig. 10. Calculated and actual concentrations for the 2000 Rhine data: (a) dissolved concentrations (surface water layer); (b) ratio of dissolved A<sub>9</sub>PEC and A<sub>9</sub>PEO; (c) concentrations in SPM; (d) concentrations in sediment. ×, actual A<sub>9</sub>PE<sub>1,2</sub>C; + and dotted line, calculated profile; ▲, actual A<sub>9</sub>PE<sub>>2</sub>C; △ and solid line, calculated profile; ●, actual NP; ○ and dotted line, calculated profile; ■, actual A<sub>9</sub>PEO<sub>>2</sub>; □ and striped line, calculated profile; ◆, actual A<sub>9</sub>PEO<sub>1,2</sub>; ◇ and striped/dotted line, calculated profile; \*, actual A<sub>9</sub>PEC/A<sub>9</sub>PEO ratio; striped line, calculated ratio.

the estuary, it was hypothesized that the canal Gent–Terneuzen could be a relevant point source of A<sub>9</sub>PEO and metabolites to the Scheldt estuary (Jonkers et al., 2003). Therefore, the significance of this additional source was evaluated.

When concentrations in the canal were set to 0, the decrease in the fit of the dissolved profiles was significant for all analytes (Table 6, scenario VII). When concentrations in the canal were increased, a 3-fold increase was necessary to obtain a significant deviation from the optimum scenario for all analytes (Table 6, scenario VIII).

It is concluded that the canal discharge does have a significant influence on the concentration profiles in the estuary.

### 3.3.4. Sensitivity towards biodegradation

Different biodegradation rates were tested to evaluate the influence of this process on the calculated concentration profiles of 1999 in the Scheldt estuary. The results in Fig. 11b show that for A<sub>9</sub>PEO<sub>>2</sub> changes in

the biodegradation rates had a relatively strong effect on the profiles. In Table 6, the quality of the fits are listed for scenarios with the degradation rates for all compounds changed to 0, 0.5 or 2 times the optimum values (scenarios IX, X and XI, respectively).

For all concentration profiles of the optimum scenario, the calculated concentrations were higher than the actual values in the upper part, and lower than the actual values in the lower part of the estuary. This may indicate that for each analyte, the biodegradation rate used in the model was too low in the relatively fresh part and too high in the saline part of estuary, and that the biodegradation rate is salinity dependent. Bacterial activity is usually lower in waters with higher salinity, as has also been shown for the biodegradation rates of surfactants in several publications (Terzic et al., 1992; Gonzalez-Mazo et al., 1997). Kveřtak et al. (1994) reported a salinity dependent biodegradation of A<sub>9</sub>PEO in a stratified estuary. They observed that biodegradation rates can be up to 8.5 times higher in the surface water layer than in the lower saline layer.

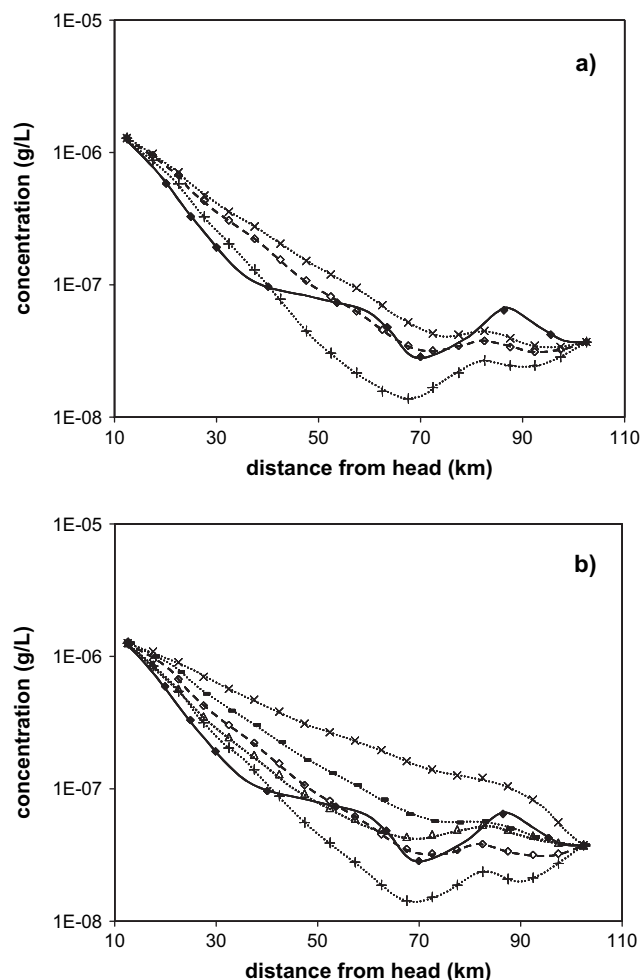


Fig. 11. (a) Actual and calculated dissolved concentration profiles of  $A_9PEO_{>2}$  using different sorption coefficients for the 1999 Scheldt model.  $\blacklozenge$  and solid line, actual concentration profile;  $\diamond$  and striped line, optimum model scenario ( $K_d = 47000$ );  $\times$ , sorption coefficient set to 0;  $+$ , sorption coefficient 5 times the optimum value ( $K_d = 235000$ ). (b) Actual and calculated dissolved concentration profiles using different biodegradation rate constants for the 1999 Scheldt model for  $A_9PEO_{>2}$ .  $\blacklozenge$  and solid line, actual concentration profile;  $\diamond$  and striped line, optimum model scenario;  $\times$ , biodegradation rate set to 0;  $+$ , biodegradation rate  $\times 1.5$  ( $0.092 \text{ day}^{-1}$ );  $-$ , biodegradation rate  $\times 0.5$  ( $0.031 \text{ day}^{-1}$ );  $\triangle$ , salinity dependent biodegradation rate ( $0.001\text{--}0.183 \text{ day}^{-1}$ ).

Therefore, a model scenario was tested with salinity dependent biodegradation rates, according to an empirically derived formula:

degradation rate

$$= \text{optimum rate} \times \left( 3 - 3.07 \times \sqrt{\frac{\text{salinity}}{35}} \right)$$

With this formula, biodegradation rates are 3 times the “optimum value” at the river end, and 0.01 times the “optimum” at the sea end of the estuary. This resulted in a slight but significant improvement of the fits, as shown in Fig. 11b and Table 6 (scenario XII).

An alternative explanation for the higher degradation rates at the river end of the Scheldt estuary could be that the biodegradation rate is concentration dependent.

#### 4. Conclusions

The present study investigated the behavior of  $A_9PEO$  in two estuaries with different hydrological characteristics. The field data indicated biodegradation to be an important process in the Scheldt estuary, showed that  $A_9PEO$  is vertically stratified in the Rhine estuary and suggested that relevant additional sources of  $A_9PEO$  were present in the latter estuary.

These findings were investigated in a more quantitative way by using different model scenarios. The hydrodynamic model was able to describe the movement of water and SPM satisfactorily for both estuaries. The sorption coefficients applied in the model yielded concentrations in SPM and sediment in the same order of magnitude as the field data. By fitting the calculated dissolved concentration profiles to the profiles observed in the field, an estimation of the field biodegradation rate constants for  $A_9PEO$  and metabolites could be made. The model calculations suggest an additional input of  $A_9PEO$  and metabolites from sources in the Rotterdam harbor area amounting to 20–100% of the input from that at the head of the estuary for the different analytes.

The model revealed that the main factors governing the fate of  $A_9PEO$  in the two investigated estuaries were biodegradation in the Scheldt estuary, and the input from additional sources in the Rhine estuary.

The accumulation of  $A_9PEO$  at water surfaces deserves more attention in future risk assessment studies, as the exposure to these compounds will be either considerably higher or lower than predicted from average concentrations for different organisms dwelling at or below the water surface.

#### Acknowledgements

The Dutch Ministry of Transport, Public Works and Water Management (RIKZ) is acknowledged for arranging the availability of the research ships. The crew of the research ships Argus and Cygnus are thanked for making the sampling campaigns possible, and the colleagues and students of the MTC department for their assistance during sampling. The authors want to thank the scientists at the RIKZ laboratory Middelburg for performing the analyses of the standard parameters of all water and sediment samples, and Dik Ludikhuizen (RIZA), Koos Doekes (RIKZ) and Dr. Ruud Steen for providing hydrological data on the Scheldt and Rhine estuaries.  $A_9PEO$  and  $A_9PEC$  standards were kindly provided by Dr. Francesc

Ventura, AGBAR, Spain, and the Shell Laboratory, Amsterdam, The Netherlands. This work was financially supported by the RIKZ institute of the Dutch ministry of Transport, Public Works and Water Management, project MONOS, and the European Union, project PRISTINE (ENV4-CT97-0494).

## References

- Ahel, M., Hrsak, D., Giger, W., 1994. Aerobic transformation of short-chain alkylphenol polyethoxylates by mixed bacterial cultures. *Archives of Environmental Contamination and Toxicology* 26, 540–548.
- Amano, K., Fukushima, T., Nakasugi, O., 1991. Fate of linear alkylbenzene sulfonates in a lake estuary. *Water Science and Technology* 23, 497–506.
- Baeyens, W.F.J., Van Eck, B., Lambert, C., Wollast, R., Goeyens, L., 1998. General description of the Scheldt estuary. *Hydrobiologia* 366, 1–14.
- Bennie, D.T., 1999. Review of the environmental occurrence of alkylphenols and alkylphenol ethoxylates. *Water Quality Research Journal of Canada* 34, 79–122.
- Boderie, P.M.A., Sonneveldt, H.L.A., 1996. Emissie-Immissie analyse van het Rotterdamse havengebied. Waterloopkundig Laboratorium report no. T1493.01.
- Cox, P., Drys, G., 2003. Directive 2003/53/EC of the European Parliament and of the council. Official Journal of the European Communities, 17.7.2003, document L178.
- De Beer, K., Van der Wielen, F.W.M., Kiewiet, A.T., De Voogt, P., 1996. Analysis of alkylphenols and alkylphenol ethoxylates in marine sediments (DIFFCHEM). Internal report. University of Amsterdam, Department of Environmental Chemistry, Amsterdam, The Netherlands.
- DiCorcia, A., Costantino, A., Crescenzi, C., Marinoni, E., Samperi, R., 1998. Characterization of recalcitrant intermediates from biotransformation of the branched alkyl side chain of nonylphenol ethoxylate surfactants. *Environmental Science and Technology* 32, 2401–2409.
- Eisma, D., Laane, R., Cadée, G., 1982. Supply of suspended matter and particulate and dissolved organic carbon from the Rhine to the coastal North Sea. *Mitteilungen aus dem Geologisch-Paläontologischen Institut Universität Hamburg* 52, 483–505.
- Fenner, K., Kooijman, C., Scheringer, M., Hungerbühler, K., 2002. Including transformation products into the risk assessment for chemicals: the case of nonylphenol ethoxylate usage in Switzerland. *Environmental Science and Technology* 36, 1147–1154.
- Ferguson, P.L., Iden, C.R., Brownawell, B.J., 2001. Distribution and fate of neutral alkylphenol ethoxylate metabolites in a sewage-impacted urban estuary. *Environmental Science and Technology* 35, 2428–2435.
- Gonzalez-Mazo, E., Honing, M., Barceló, D., Gomez-Parra, A., 1997. Monitoring long-chain intermediate products from the degradation of linear alkylbenzene sulfonates in the marine environment by solid-phase extraction followed by liquid chromatography ionspray mass spectrometry. *Environmental Science and Technology* 31, 504–510.
- Harris, J.R.W., Gorley, R.N., 1998. An Introduction to Modelling Estuaries with ECoS 3. NERC, Plymouth, UK, pp. 23–27.
- Heemken, O.P., Reincke, H., Stachel, B., Theobald, N., 2001. The occurrence of xenoestrogens in the Elbe river and the North Sea. *Chemosphere* 45, 245–259.
- Jobling, S., Sumpter, J.P., 1993. Detergent components in sewage effluent are weakly estrogenic to fish – an in-vitro study using rainbow-trout (*Oncorhynchus mykiss*) hepatocytes. *Aquatic Toxicology* 27, 361–372.
- Jonkers, N., De Voogt, P., 2003. Nonionic surfactants in marine and estuarine environments. In: Knepper, T.P., Barceló, D., De Voogt, P. (Eds.), *Analysis and Fate of Surfactants in the Aquatic Environment*. Elsevier, Amsterdam, pp. 719–747.
- Jonkers, N., Knepper, T.P., De Voogt, P., 2001. Aerobic biodegradation studies of nonylphenol ethoxylates in river water using liquid chromatography–electrospray tandem mass spectrometry. *Environmental Science and Technology* 35, 335–340.
- Jonkers, N., Laane, R.W.P.M., De Voogt, P., 2003. Fate of nonylphenol ethoxylates and their metabolites in two Dutch estuaries: evidence of biodegradation in the field. *Environmental Science and Technology* 37, 321–327.
- Jonkers, N., Laane, R.W.P.M., De Voogt, P. Sources and fate of nonylphenol ethoxylates and their metabolites in the Dutch coastal zone. *Marine Chemistry*, submitted for publication.
- Knepper, T.P., Berna, J.L., 2003. Surfactants: properties, production, and environmental aspects. In: Knepper, T.P., Barceló, D., De Voogt, P. (Eds.), *Analysis and Fate of Surfactants in the Aquatic Environment*. Elsevier, Amsterdam, pp. 1–45.
- Kvešták, R., Ahel, M., 1995. Biotransformation of nonylphenol polyethoxylate surfactants by estuarine mixed bacterial cultures. *Archives of Environmental Contamination and Toxicology* 29, 551–556.
- Kvešták, R., Terzić, S., Ahel, M., 1994. Input and distribution of alkylphenol polyethoxylates in a stratified estuary. *Marine Chemistry* 46, 89–100.
- Legler, J., Van den Brink, C.E., Brouwer, A., Murk, A.J., Van der Saag, P.T., Vethaak, A.D., Van der Burg, B., 1999. Development of a stably transfected estrogen receptor-mediated luciferase reporter gene assay in the human T47D breast cancer cell line. *Toxicological Sciences* 48, 55–66.
- Liu, Y.P., Millward, G.E., Harris, J.R.W., 1998. Modeling the distributions of dissolved Zn and Ni in the Tamar estuary using hydrodynamics coupled with chemical kinetics. *Estuarine, Coastal and Shelf Science* 47, 535–546.
- Marcomini, A., Pojana, G., Sfriso, A., Quiroga Alonso, J.M., 2000. Behavior of anionic and nonionic surfactants and their persistent metabolites in the Venice lagoon, Italy. *Environmental Toxicology and Chemistry* 19, 2000–2007.
- Morioka, T., Chikami, S., 1986. Basin-wide ecological fate model for management of chemical hazards. *Ecological Modelling* 31, 267–281.
- Peters, R.J.B., 2003. Hazardous chemicals in precipitation. TNO-report R2003/198, Apeldoorn, The Netherlands.
- Petrovic, M., Fernández-Alba, A.R., Borull, F., Marce, R.M., González-Mazo, E., Barceló, D., 2002. Occurrence and distribution of nonionic surfactants, their degradation products, and linear alkylbenzene sulfonates in coastal waters and sediments in Spain. *Environmental Toxicology and Chemistry* 21, 37–46.
- Pham, M.K., Martin, J.M., Garnier, J.M., Li, Z., Boutier, B., Chiffolleau, J.F., 1997. On the possibility of using the commercially available ECoS model to simulate Cd distribution in the Gironde estuary (France). *Marine Chemistry* 58, 163–172.
- Potter, T.L., Simmons, K., Wu, J.N., Sanchez-Olvera, M., Kosteki, P., Calabrese, E., 1999. Static die-away of a nonylphenol ethoxylate surfactant in estuarine water samples. *Environmental Science and Technology* 33, 113–118.
- Pritchard, D.W., 1958. Salt balance and exchange rate for Chincoteague Bay. *Journal of Marine Research* 17, 412–423.
- Shang, D.Y., Macdonald, R.W., Ikonou, M.G., 1999. Persistence of nonylphenol ethoxylate surfactants and their primary degradation products in sediments from near a municipal outfall in the strait of Georgia, British Columbia, Canada. *Environmental Science and Technology* 33, 1366–1372.
- Soetaert, K., Herman, P.M.J., 1995. Estimating estuarine residence times in the Westerschelde (The Netherlands) using a box

- model with fixed dispersion coefficients. *Hydrobiologia* 311, 215–224.
- Steen, R.J.C.A., van der Vaart, J., Hiep, M., van Hattum, B., Cofino, W.P., Brinkman, U.A.Th., 2002. Net fluxes of pesticides from the Scheldt estuary into the North Sea: a model approach. *Environmental Pollution* 116, 75–84.
- Terzic, S., Hrsak, D., Ahel, M., 1992. Primary biodegradation kinetics of linear alkylbenzene sulfonates in estuarine waters. *Water Research* 26, 585–591.
- Van Eck, G.T.M., De Rooij, N.M., 1990. Development of a water quality and bio-accumulation model for the Scheldt estuary. In: Michaelis, W. (Ed.), *Coastal and Estuarine Studies*. Springer Verlag, Berlin, Germany.
- Van Gils, J.A.G., Ouboter, M.R.L., De Rooij, N.M., 1993. Modelling of water and sediment quality in the Scheldt estuary. *Netherlands Journal of Aquatic Ecology* 27, 257–265.
- Van Maldegem, D.C., Mulder, H.P.J., Langerak, A., 1993. A cohesive sediment balance for the Scheldt estuary. *Netherlands Journal of Aquatic Ecology* 27, 247–256.
- Van Ry, D.A., Dachs, J., Gigliotti, C.L., Brunciak, P.A., Nelson, E.D., Eisenreich, S.J., 2000. Atmospheric seasonal trends and environmental fate of alkylphenols in the lower Hudson River Estuary. *Environmental Science and Technology* 34, 2410–2417.
- Van Vlaardingen, P., Posthumus, R., Traas, T.P., 2003. Environmental risk limits for alkylphenols and alkylphenol ethoxylates. National Institute of Public Health and the Environment, report 601501019, Bilthoven, The Netherlands.
- Vuksanovic, V., De Smet, F., van Meerbeeck, S., 1996. Transport of polychlorinated biphenyls (PCB) in the Scheldt Estuary simulated with the water quality model WASP. *Journal of Hydrology* 174, 1–18.
- Ying, G.G., Williams, B., Kookana, R., 2002. Environmental fate of alkylphenols and alkylphenol ethoxylates: a review. *Environment International* 28, 215–226.
- Zwolsman, J.J.G., 1999. Geochemistry of trace metals in the Scheldt estuary. Ph. D. Thesis. Universiteit Utrecht, The Netherlands.